

## **Neurobehavioral Indices of Gaze Perception are Associated with Social Cognition across Schizophrenia Patients and Healthy Controls: Supplemental Information**

### **Supplemental Methods**

#### **Dataset description**

Inclusion criteria included the following: age 18 to 55 years old; capable of giving informed consent; normal or corrected-to-normal vision; no significant medical or neurological illness; no history of closed head injury with neurological sequela; no current pregnancy; no contraindications to MRI (e.g., metal objects in the body); and no alcohol/substance abuse in the past month or dependence in the past 6 months. Additional *exclusion* criteria for HC included: past or current Axis I disorder; history of psychotic or bipolar disorder among first-degree relatives; and current Beck Depression Inventory (BDI-II) (Beck & Steer, 1993) score  $> 8$ .

As noted in the main text, of the 148 participants with behavioral data, 116 had valid fMRI data (62 SZ, 54 HC). A total of 14 participants completed only the clinical assessment and behavioral measures of social cognition, not returning for the fMRI scanning session. A total of 7 participants did not have field-map scan data available for preprocessing, 2 participants were missing anatomical scans, and 2 participants did not have enough valid functional scan runs due to equipment malfunction or lack of behavioral responding. Finally, 7 participants were excluded for excessive head motion (having a mean framewise displacement  $> 0.40$  mm (Power et al., 2015)).

As noted in the main text, the dataset was made up of two different subsamples, which used slightly different protocols. These two protocols were from two separate grant projects; the first one was an institutional grant and the second one funded by the NIMH. By the time the second grant was reviewed at NIMH, multiband fMRI acquisition became the new standard in

the field and reviewers recommended an updated scanning protocol. The two scanning protocols are detailed below.

### **fMRI data acquisition for first subsample**

MRI scanning in both subsamples occurred on a 3.0 T GE MR 750 Discovery scanner (LX [8.3] release, General Electric Healthcare, Buckinghamshire, United Kingdom). The first scanning protocol was used for a subsample of 49 participants (27 SZ, 22 HC). A T1-weighted image was acquired in the same prescription as the functional images to facilitate co-registration. Functional images were acquired with a T2\*-weighted, reverse spiral acquisition sequence with excellent signal recovery in areas of high susceptibility to artifacts (gradient echo, TR=2000 ms, TE=30 ms, FA=90 degrees, FOV=22 cm, 40 slice, 3mm thick/0mm skip, equivalent to  $64 \times 64$  voxel grid). Participants underwent 3 runs, with each run containing 12 task blocks and 11 fixation blocks. Within each task block, the gaze angle and gender of face stimuli were pseudo-randomized. Each face was presented for 1.5s and separated from the next face by a random jitter (1.6 – 3.9 s). There was a total of 108 trials (6 trials  $\times$  6 blocks  $\times$  3 runs) for each task (Eyes and Gender). Each run had 228 volumes (plus 4 initial, discarded volumes to allow for equilibration of the scanner signal) with isotropic voxels 3 mm on edge. After acquisition of functional volumes, a high-resolution T1 scan (Ax F SPGR, FOV=26 cm, TI=500 ms, FA=15 degree, BW=31.25,  $256 \times 256$  matrix, 128 slices, 1.2 mm interleaved with no skip) was obtained for anatomic normalization.

### **fMRI data acquisition for second subsample**

A second scanning protocol was used for a subsample of 67 participants (35 SZ, 32 HC). A T1-weighted image was acquired in the same prescription as the functional images to facilitate co-registration. Functional images were acquired with a T2\* - weighted multi-band EPI sequence

(gradient echo, multiband acceleration factor of 8, TR=800 ms, TE=30 ms, FA=52 degrees, FOV=23 cm, 60 slice, 2.4mm thick/0mm skip, equivalent to  $96 \times 96$  voxel grid). Participants underwent 6 runs, with each run containing 6 task blocks and 5 fixation blocks. Within each block, the gaze angle and gender of face stimuli were pseudo-randomized. Each face was presented for 1.5s and separated from the next face by a random jitter (1.6 – 3.9 s). There was a total of 216 trials (6 trials  $\times$  6 blocks  $\times$  6 runs) for each task (Eyes, Gender). Each run had 275 volumes (plus 12 initial, discarded volumes to allow for equilibration of scanner signal) with isotropic voxels 2.4 mm on edge. After acquisition of functional volumes, a high-resolution T1w scan (MPRAGE, FOV=25.6 cm, TI=1060 ms, FA=8 degree, BW=31.25,  $320 \times 320$  matrix, 208 slices, 0.8 mm interleaved with no skip) was obtained for anatomic normalization.

### **fMRI data preprocessing**

fMRI data were processed using typical methods in Statistical Parametric Mapping (SPM12, Wellcome Institute of Cognitive Neurology, London). Slice-time correction was done using sinc-interpolation, weighted by a Hanning kernel in time. Then all scans were realigned to the 10th volume acquired during each scan. The time series of functional volumes were then co-registered with the high-resolution T1 image, spatially normalized to the MNI152 brain, and spatially smoothed with an 8 mm isotropic Gaussian kernel.

### **fMRI Data Modeling**

First-level analysis began with applying a high-pass filter (128 s) to the anatomically normalized time series and then regressing the time series on regressors convolved with a canonical hemodynamic response function. The regressors included 2 regressors of interest (Gaze trials, Gender trials) and 27/30 nuisance regressors including 24 motion parameters (6 for each translation/rotation direction, their quadratic terms, and first and second derivatives), as

well as 3 runs for the first subsample and 6 runs for the second subsample. For all second-level analyses, subsample and mean framewise displacement were included as covariates, but results did not substantively differ if these covariates were omitted. Second-level analyses were initially computed for six contrasts: all-trials vs. baseline, gaze vs. baseline, gender vs. baseline, gaze vs. gender, modulation by participants' perception of stimuli as self-directed, and modulation by stimulus gaze angle. We chose not to report results for gaze vs. baseline or gender vs. baseline contrasts in the main text, due to their similarity to one another and to the all-trials vs. baseline contrast; likewise, we did not extract beta estimates from the individual gaze/gender vs. baseline contrasts.

### **Behavioral Data and Latent Variable Analysis**

Threshold and width for the gaze task were estimated using hierarchical Bayesian modeling implemented using the *psignifit 4* toolbox (Schütt et al., 2016), with default priors. For our behavioral latent variable model, Bayesian estimation was used, which provides the most robust estimation of associations among latent and observed variables (Muthén & Muthén, 2017). Estimation relied upon default priors and was implemented using a Markov Chain Monte Carlo (MCMC) algorithm based on the Gibbs sampler. For neural latent variable model estimation, we used full-information robust weighted least squares estimation (WLSMV), which is recommended for models including categorical variables. Bayesian estimation was not used, as MPLUS does not support exploratory factors with Bayesian estimation. An oblimin rotation with  $\gamma = 0$  was used for estimating our exploratory latent neural factors. In our neural model, loadings and residual correlations for our social cognition latent variable were fixed to the values obtained using Bayesian estimation. Fit indices were computed for both models, including root mean

square error of approximation (RMSEA), Comparative Fit Index (CFI), and Tucker Lewis Index (TLI).

For follow-up moderation analyses, regression models with estimated factor scores were computed rather than using separate latent variable analyses, due to 1) the relatively small sample size within each diagnostic group and 2) because multi-group SEM and statistical interactions cannot be implemented in MPLUS models also using exploratory factors and WLSMV. Estimated factor scores for social cognition were computed based on our Bayesian model of social cognition, gaze perception, and diagnosis. (Factor scores were computed as the mean of plausible values derived using Bayesian sampling with 100,000 draws.) Estimated factor scores for each of the six neural factors were computed based on our WLSMV models. (Neural factor scores were computed using the regression method.) Finally, variables were computed to quantify two-way interactions of diagnosis with the two gaze performance metrics and six neural factors; each variable was converted to a z-score and then multiplied by the dummy coded scores for diagnosis, and the resulting interaction terms were converted to z-scores, which were then used as interaction terms in subsequent regression models.

For follow-up sensitivity analyses using additional covariates, we ran additional versions of our original behavioral and neural models. First, a behavioral model with Bayesian estimation was computed, which examined correlations among gaze width, gaze threshold, diagnosis, and latent social cognition, when each of these variables was regressed on the covariates of age, sex, cognitive ability, and subsample. Then, a neural model with WLSMV estimation was computed, which included age, sex, cognitive ability, and subsample as additional regressors that were allowed to predict social cognition, diagnosis, gaze width, and gaze threshold; correlations were freely estimated among the three covariate variables and between the covariates and our latent

neural factors. Next, behavioral and neural models were estimated that excluded task-performance datapoints identified as outliers using Rosner's generalized ESD test (Rosner, 1983). Finally, at the suggestion of reviewers, we estimated additional models including only ER-40, RME, and the perceiving emotions branch score from the MSCEIT as indicators of social cognition; again, the behavioral and neural models were estimated using Bayesian and WLSMV estimators, respectively. Fit indices for these follow-up models are presented in Table S8.

### **Supplemental Results**

Second-level analyses across all participants revealed voxel clusters with significantly different activation between task vs. baseline, significantly different activation between gaze and gender conditions, modulation of activation by participants' individual perception of stimuli as self-directed vs. averted, and modulation of activation by viewing stimuli with more objectively self-directed vs. averted gaze angles. Significant clusters were observed in various brain regions canonically associated with social cognition (e.g., insula/inferior frontal gyrus, dorsomedial prefrontal cortex, inferior parietal lobule/angular gyrus, temporoparietal junction/superior temporal gyrus/superior temporal sulcus, posterior cingulate/precuneus, amygdala, and fusiform gyrus), as well as in regions associated with vision (e.g., cuneus, middle occipital gyrus, and lingual gyrus) and sensorimotor function (supplementary motor area, premotor cortex, pre-central/post-central gyrus, and cerebellum). Significant clusters are visualized in Figures S4–S9 and are presented with coordinates and t-statistics in Table S2. Similar results were obtained across contrasts, despite some differences in quantity, location, and size of clusters.

Significant differences between groups were found for a cluster within left pre-/post-central gyrus, for the task vs. baseline contrast (as well as for gaze vs. baseline and gender vs. baseline contrasts); these are visualized in Figures S10–S12 and reported in Table S3. No

significant between-group differences were found for the other contrasts (gaze vs. gender, modulation by perception as self-directed vs. averted, and modulation by objective gaze angle); group-specific activation maps for these contrasts are presented in Figures S13–S15.

### **Supplemental Discussion**

#### **Basic Neural Correlates of Gaze Perception**

Our fMRI data showed that gaze perception, relative to general face processing, in both SZ and HC, preferentially activates insula, dmPFC, and IPL—regions with documented roles in gaze perception and social cognition (Cavallo et al., 2015; Tso et al., 2018). These findings serve as successful validation of our task’s basic effects. Gaze processing involves a wide range of neural processes, spanning basic visual processing in early visual cortex (e.g., V1, V2), analysis of eye gaze direction in the STS (Carlin et al., 2011; Caruana et al., 2014; Sato et al., 2016; Steuwe et al., 2014; Schobert et al., 2018; Boyarskaya et al., 2015), and visuospatial encoding of gaze direction and re-orientating attention in the parietal cortex, especially the IPL (Itier & Batty, 2009). Additionally, higher-order processes in a number of frontal regions have also been implicated, including the dmPFC/ACC (Calder et al., 2002; Schilbach et al., 2006; Urakawa et al., 2015), precentral gyrus (Cavallo et al., 2015; Grosbras et al., 2005; Hooker et al., 2003), and the middle/inferior frontal gyrus (Bristow et al., 2007; Cavallo et al., 2015). Anterior medial regions such as mPFC and ACC are known for action monitoring, cognitive control, self-referential processing, and theory of mind (Amodio & Frith, 2006; Meyer & Lieberman, 2018). The regions adjacent to the central sulcus (i.e., the pre- and post-central gyri) represent the core motor control system and partially the mirror neuron system (Rizzolatti & Craighero, 2004). Involvement of these frontal brain regions suggests that gaze processing may inherently involve the assessment of self-relatedness of the gaze, evaluation of the mental state of the owner of the

gaze, tendency to shift gaze or take actions in response to the seen gaze, and general cognitive and motor control to regulate these processes. These results can also be further understood through the lens of network neuroscience and work on individual differences.

### **Relevance of Network Approaches and Individual Differences Research**

Our neuroimaging results also connect well with research from a network approach, which suggests the default and salience networks—and their constituent nodes such as the insula, TPJ, ACC, STS, IPL, dmPFC, and PCC—are particularly important substrates of social cognition and associated individual differences; many of the regions identified in our current findings overlap with key nodes of these networks. Multiple authors have noted similarities between the brain’s default network and networks associated with social cognition (Mars et al., 2012; Meyer, 2019; Schilbach et al., 2008; Spreng & Andrews-Hanna, 2015), with some proposing that this indicates the human brain is “social by default” (Meyer, 2019; Schilbach et al., 2008). Nonetheless, it is important to note that the default network also plays important roles beyond social cognition, most of which seem to involve internal simulation and self-generated thought (Andrews-Hanna et al., 2014; Blain et al., 2020; Buckner et al., 2008; Spreng et al., 2009; Tamir et al., 2016).

Theories regarding the social brain and default network—paired with the present findings—also connect well with neuroimaging research from personality and individual difference perspectives. For instance, individual differences in social cognitive ability have been linked to strength of neural response to social stimuli in the default network—particularly in the dmPFC (Udochi et al., 2022)—and to functional connectivity between default network subsystems (Allen et al., 2017). Likewise, self-report measures related to social functioning have been linked to individual differences in various properties of the default network and its



constituent nodes, including task-based activation (Udochi et al., 2022), functional connectivity (Abram et al., 2017; Allen et al., 2017; Meda et al., 2014; Takeuchi, Taki, Nouchi, et al., 2014), structural connectivity (Takeuchi et al., 2013, 2019), and regional volume (Eres et al., 2015; Lewis et al., 2011; Takeuchi, Taki, Sassa, et al., 2014). Nonetheless, as reflected in the current results, the default network is not the only important neural substrate of social cognition, as regions such as the insula and ACC—canonically more associated with the salience or ventral attention networks—and sensorimotor regions are also essential (Decety, 2015; Green et al., 2015; Singer et al., 2009; Tso et al., 2018). Indeed, other work has linked individual differences in social-related measures to properties of the salience network and its constituent nodes such as the ACC and insula (Bernhardt et al., 2014; Hou et al., 2017). Future studies could utilize network-based analyses to more directly elucidate how these networks—as well as their interactions and reconfiguration across different task modalities—might contribute to social cognition and associated individual differences.

**Table S1***Group Differences for Individual Social Cognition Tasks*

	SZ (n = 77) Mean ± SD	HC (n = 71) Mean ± SD	t or $\chi^2$	p	Cohen's d
MSCEIT Perception	.58 ± .14	.64 ± .09	-3.0	.003	0.51
MSCEIT Using	.45 ± .08	.49 ± .05	-3.5	< .001	0.60
MSCEIT Understanding	.55 ± .17	.66 ± .10	-4.9	< .001	0.79
MSCEIT Managing	.40 ± .11	.47 ± .05	-4.6	< .001	0.82
Gaze Threshold	.68 ± .18	.75 ± .14	-2.3	.022	0.43
Gaze Width	1.1 ± 0.7	0.7 ± 0.5	3.4	< .001	0.66
RME	.69 ± .12	.78 ± .10	-3.9	< .001	0.81
ER-40	31.1 ± 5.9	34.3 ± 2.5	-3.3	.002	0.71

*Note.* MSCEIT = Mayer-Salovey-Caruso Emotional Intelligence Test, RME = Reading the Mind in the Eyes Test, ER-40 = Penn Emotion Recognition Task.

**Table S2***Significant clusters from full-sample, second-level analyses*

Cluster Label	# Voxels	Cluster $p$ FDR-corr	Peak MNI Coordinates	Peak $T$ -value
<b>All Trials</b>				
<b>Positive</b>				
R_Cerebellum	22372	< .001	[32, -54, -29]	24.61
R_IPL	1303	< .001	[32, -50, 43]	14.19
R_CorpusCallosum	31	.005	[6, -26, 26]	5.71
L_MFG/PFC	31	.005	[-35, 46, 14]	5.48
<b>Negative</b>				
L_PCC/Precuneus	13725	< .001	[-11, -57, 14]	19.11
L_SFG/PFC	4853	< .001	[-23, 27, 40]	18.13
R_MFG/PFC	524	< .001	[25, 30, 40]	15.10
L_Hippocampus	670	< .001	[-30, -40, -10]	14.73
L_STG	2163	< .001	[-56, -11, -3]	12.98
R_Fusiform	186	< .001	[30, -42, -10]	12.36
R_LingualGyrus	140	< .001	[13, -74, -3]	11.33
L_Pre/PostCentral	186	< .001	[-40, -16, 33]	9.02
R_Hippocampus	20	.012	[28, -18, -20]	6.58
<b>Gaze Main Effect</b>				
<b>Positive</b>				
R_Cerebellum	23197	< .001	[32, -54, -29]	24.16
R_IPL	1528	< .001	[32, -47, 43]	15.97
L_OFC	165	< .001	[-47, 44, -12]	7.14
R_STG	77	< .001	[49, -57, 9]	6.02
R_ACC	14	.045	[4, 3, 28]	6.00
R_CorpusCallosum	25	.009	[6, -26, 26]	5.93
<b>Negative</b>				
L_PCC/Precuneus	13980	< .001	[-8, -57, 14]	20.74
L_MFG/PFC	4214	< .001	[-20, 27, 40]	18.71

L_STG	2108	< .001	[-56, -11, -3]	14.41
R_MFG/PFC	503	< .001	[23, 30, 43]	14.27
R_Fusiform	418	< .001	[30, -42, -10]	13.19
R_AngularGyrus	183	< .001	[44, -71, 33]	10.30
L_IFG	54	< .001	[-30, 34, -10]	8.43
L_ITG	81	< .001	[-56, -50, -10]	7.71
R_Hippocampus	41	.001	[28, -18, -20]	7.12
L_IFG	35	.001	[-47, 30, 4]	6.76
<b>Gender Main Effect</b>				
<b>Positive</b>				
R_Cerebellum	7560	< .001	[32, -52, -27]	22.28
L_SMA	8237	< .001	[-6, 1, 52]	17.02
R_IPL	814	< .001	[32, -52, 45]	10.54
R_MFG	2135	< .001	[37, 1, 62]	10.38
R_Hippocampus	152	< .001	[23, -28, -5]	9.00
<b>Negative</b>				
L_Extrastriate	12294	< .001	[-37, -81, 33]	17.53
L_ACC	3111	< .001	[-6, 42, -3]	14.54
L_SFG	664	< .001	[-23, 27, 40]	13.88
L_Hippocampus	302	< .001	[-30, -40, -10]	12.88
R_MFG	422	< .001	[25, 30, 40]	12.85
R_Hippocampus	135	< .001	[30, -40, -10]	10.42
L_MTG	1770	< .001	[-54, -9, -12]	9.96
R_LingualGyrus	87	< .001	[13, -74, -3]	9.47
L_IFG	401	< .001	[-47, 30, 4]	9.18
L_Pre/PostCentral	124	< .001	[-40, -16, 33]	8.19
L_LingualGyrus	68	< .001	[-13, -76, -5]	7.82
R_Insula/IFG	30	.006	[32, 13, -17]	5.94
<b>Gaze vs. Gender Contrast</b>				
<b>Positive</b>				
R_Insula/IFG	3509	< .001	[35, 20, -3]	12.47
L_Insula/IFG	457	< .001	[-32, 20, -3]	11.40

R_IPL/IntraparietalSulcus	874	< .001	[37, -47, 48]	11.13
R_dmPFC/SMA	657	< .001	[4, 18, 50]	9.84
R_STG/STS/TPJ/V5	1116	< .001	[44, -57, 12]	9.72
L_Cerebellum	463	< .001	[-8, -74, -29]	9.59
R_IOG	260	< .001	[32, -90, -3]	8.27
R_Thalamus	94	< .001	[11, -16, 12]	7.52
L_STG/STS/TPJ	172	< .001	[-44, -57, 14]	6.70
R_Cerebellum	28	.009	[1, -54, -36]	6.54
L_OFC	163	< .001	[-49, 42, -8]	6.52
L_MOG/V2	68	< .001	[-30, -93, -3]	6.50

**Negative**

L_dIPFC/SFG	322	< .001	[-20, 30, 43]	8.54
R_PCC/Precuneus	357	< .001	[1, -64, 26]	7.35
L_PCC	64	< .001	[-4, -40, 36]	7.31
L_LingualGyrus/V2	273	< .001	[-20, -78, -8]	7.30
L_AngularGyrus	213	< .001	[-42, -66, 36]	7.06
R_STG/STS	59	.001	[64, -6, -12]	7.00
R_STG/STS	385	< .001	[66, -21, 14]	6.59
R_LingualGyrus/V2	166	< .001	[18, -71, -3]	6.51
R_vmPFC/ACC	100	< .001	[1, 46, -5]	6.27
R_mPFC/SFG	19	.028	[20, 30, 48]	5.92
L_PostCentral	90	< .001	[-61, -21, 21]	5.87

**Participant Perception Modulation****Positive**

L_Insula/IFG	669	< .001	[-40, 18, -5]	8.82
R_Insula/IFG	2162	< .001	[42, 20, -5]	8.54
R_dmPFC/SFG	1122	< .001	[6, 42, 40]	7.45
R_STS/STG/TPJ	156	< .001	[54, -35, -3]	6.98
R_Amygdala/Hippocampus	27	.013	[18, -4, -15]	6.73
R_IntraparietalSulcus/IPG	62	< .001	[44, -45, 48]	5.87
L_AngularGyrus	69	< .001	[-59, -59, 31]	5.67
R_AngularGyrus	25	.015	[52, -62, 45]	5.36

**Negative**

L_Fusiform	40	.003	[-20, -86, -8]	6.43
L_Pre/PostCentral	92	< .001	[-40, -23, 60]	6.27
L_SPG/Precuneus	23	.014	[-16, -69, 50]	5.76
L_Precuneus	15	.032	[-11, -52, 60]	5.20

**Gaze Angle Modulation****Positive**

L_Insula/IFG	358	< .001	[-37, 18, -3]	9.41
R_dmPFC/SFG	880	< .001	[4, 27, 50]	9.26
R_Insula/IFG	1990	< .001	[42, 20, -5]	9.06
L_OFC	65	< .001	[-47, 42, -5]	5.89

**Negative**

L_Fusiform	1595	< .001	[-20, -86, -8]	9.53
L_MOG/V2	1470	< .001	[-20, -88, 16]	8.78
R_PCC/Precuneus	167	< .001	[11, -57, 14]	8.00
R_Precentral/ROL	600	< .001	[52, -2, 7]	7.12
L_STG/STS	461	< .001	[-54, -38, 12]	7.00
L_Calcarine/Retrosplenia	243	< .001	[-16, -59, 19]	6.87
R_PCC/MidCingulate	83	< .001	[13, -28, 43]	6.84
L_PostCentral	128	< .001	[-40, -26, 57]	6.68
R_PostCentral	205	< .001	[25, -45, 64]	6.62
R_Calcarine/Retrosplenia	44	.002	[20, -47, 21]	6.55

*Note.* R = right hemisphere, L = left hemisphere, Diff = contrast of neural activity during gaze vs. gender conditions, Per = parametric modulation by participants' individual perception/behavioral endorsement of stimuli as self-directed vs. averted, Ang = parametric modulation by objective gaze angle, All = contrast of neural activity across both task conditions vs. baseline, IFG = inferior frontal gyrus, IPL = inferior parietal lobule, dmPFC = dorsomedial prefrontal cortex, SMA = supplementary motor area, STG = superior temporal gyrus, STS = superior temporal sulcus, TPJ = temporoparietal junction, V5 = middle temporal visual area, IOG = inferior occipital gyrus, OFC = orbitofrontal cortex, MOG = middle occipital gyrus, V2 = secondary visual cortex, dlPFC = dorsolateral prefrontal cortex, SFG = superior frontal gyrus, PCC = posterior cingulate cortex, vmPFC = ventromedial prefrontal cortex, ACC = anterior cingulate cortex, mPFC = medial prefrontal cortex, Hipp = hippocampus, SPG = superior parietal gyrus, MOG = middle occipital gyrus, ROL = Rolandic operculum, Retrospl = retrosplenial cortex.

**Table S3***Significant Clusters from HC vs. SZ Second-level Analyses*

Cluster Label	# Voxels	Cluster $p$ FDR-corr	Peak MNI Coordinates	Peak $T$ -value
<b>All Trials</b>				
<b>SZ &gt; HC</b>				
L_Pre/PostCentral	254	< .001	[-47, -21, 57]	7.02
<b>HC &gt; SZ</b>				
	N/A			
<b>Gaze Main Effect</b>				
<b>SZ &gt; HC</b>				
L_Pre/PostCentral	239	< .001	[-47, -18, 55]	6.85
<b>HC &gt; SZ</b>				
	N/A			
<b>Gender Main Effect</b>				
<b>SZ &gt; HC</b>				
L_Pre/PostCentral	130	< .001	[-44, -21, 55]	6.66
<b>HC &gt; SZ</b>				
	N/A			
<b>Gaze vs. Gender Contrast</b>				
<b>SZ &gt; HC</b>				
	N/A			
<b>HC &gt; SZ</b>				
	N/A			
<b>Participant Perception Modulation</b>				
<b>SZ &gt; HC</b>				
	N/A			
<b>HC &gt; SZ</b>				
	N/A			
<b>Gaze Angle Modulation</b>				
<b>SZ &gt; HC</b>				
	N/A			
<b>HC &gt; SZ</b>				
	N/A			

Table S4

*Latent Neural Factor Loadings for Model Predicting Social Cognition, Gaze Perception, and Diagnosis*

Contrast and Region of Interest	Task Activation	Gaze > Gender	Factor Label			
			Gender > Gaze	Direct Gaze	Objectively Averted Gaze	Perceived Averted Gaze
All_R_Cerebellum	0.036	-0.149	0.099	<b>0.195</b>	-0.035	-0.149
All_R_IPL	<b>0.253</b>	0.059	-0.001	0.101	0.072	0.124
All_CorpusCallosum	<b>0.481</b>	-0.090	-0.076	<b>0.288</b>	0.033	-0.080
All_L_MFG/PFC	<b>0.351</b>	-0.158	0.030	0.139	0.002	-0.047
All_L_PCC/Precuneus	<b>0.781</b>	0.094	-0.080	0.030	-0.105	-0.032
All_L_SFG/PFC	<b>0.825</b>	-0.013	-0.034	-0.015	0.004	-0.045
All_R_MFG/PFC	<b>0.826</b>	0.118	-0.088	-0.011	<b>0.129</b>	0.043
All_L_Hippocampus	<b>0.877</b>	-0.032	0.073	0.084	-0.026	-0.047
All_L_STG	<b>0.768</b>	-0.053	0.045	<b>-0.219</b>	0.023	-0.029
All_R_Fusiform	<b>0.856</b>	-0.083	0.101	0.025	-0.001	0.023
All_R_LingualGyrus	<b>0.548</b>	-0.025	-0.004	0.064	0.033	-0.006
All_L_Pre/PostCentral	<b>0.808</b>	-0.017	-0.032	-0.073	0.029	0.064
All_R_Hippocampus	<b>0.783</b>	-0.060	0.036	0.040	-0.084	-0.033
Diff_R_Insula/IFG	-0.029	<b>0.879</b>	<b>-0.189</b>	<b>0.101</b>	0.033	<b>0.119</b>
Diff_L_Insula/IFG	-0.031	<b>0.793</b>	0.014	0.037	0.014	-0.073
Diff_R_IPL/IntraparietalSulcus	-0.075	<b>0.650</b>	0.136	-0.097	-0.078	-0.002
Diff_R_dmPFC/SMA	-0.058	<b>0.776</b>	0.043	0.072	-0.099	-0.044
Diff_R_STG/STS/TPJ/V5	<b>-0.181</b>	<b>0.178</b>	<b>0.377</b>	-0.014	0.069	0.068
Diff_L_Cerebellum	0.012	<b>0.610</b>	<b>0.255</b>	0.027	-0.071	<b>-0.170</b>
Diff_R_IOG	-0.015	<b>0.306</b>	<b>0.458</b>	-0.038	-0.114	-0.180
Diff_R_Thalamus	0.005	<b>0.623</b>	<b>0.206</b>	0.006	0.061	0.001
Diff_L_STG/STS/TPJ	<b>-0.144</b>	<b>0.183</b>	<b>0.479</b>	0.000	0.049	0.160
Diff_R_Cerebellum	0.092	<b>0.426</b>	<b>0.363</b>	-0.110	-0.060	-0.116
Diff_L_OFC	-0.078	<b>0.438</b>	<b>0.282</b>	<b>0.133</b>	0.018	-0.089
Diff_L_MOG/V2	0.002	<b>0.420</b>	<b>0.375</b>	<b>-0.135</b>	-0.028	0.013
Diff_L_dIPFC/SFG	0.086	-0.038	<b>0.805</b>	<b>-0.119</b>	-0.034	0.025
Diff_R_PCC/Precuneus	-0.041	0.038	<b>0.727</b>	0.032	<b>0.156</b>	0.075
Diff_L_PCC	-0.048	0.070	<b>0.757</b>	0.099	0.066	-0.011
Diff_L_LingualGyrus/V2	-0.019	<b>0.275</b>	<b>0.469</b>	<b>-0.217</b>	0.063	0.134
Diff_L_AngularGyrus	-0.003	-0.059	<b>0.719</b>	0.064	-0.026	-0.008
Diff_R_STG/STS	-0.018	-0.030	<b>0.657</b>	0.046	<b>0.181</b>	<b>-0.129</b>



Diff_R_STG/STS	<b>-0.188</b>	<b>0.232</b>	<b>0.420</b>	-0.140	<b>0.182</b>	<b>0.144</b>
Diff_R_LingualGyrus/V2	0.042	<b>0.227</b>	<b>0.340</b>	-0.161	<b>0.205</b>	0.176
Diff_R_vmPFC/ACC	0.046	-0.006	<b>0.579</b>	<b>0.154</b>	<b>0.224</b>	0.092
Diff_R_mPFC/SFG	0.116	<b>0.312</b>	<b>0.566</b>	-0.024	-0.136	0.074
Diff_L_PostCentral	-0.052	<b>0.279</b>	<b>0.319</b>	<b>-0.213</b>	0.052	0.146
Per_L_Insula/IFG	-0.037	0.035	0.094	<b>0.814</b>	-0.042	0.160
Per_R_Insula/IFG	0.047	0.089	0.018	<b>0.716</b>	<b>-0.248</b>	0.235
Per_R_dmPFC/SFG	0.074	0.035	0.075	<b>0.675</b>	-0.123	0.327
Per_R_STS/STG/TPJ	0.037	0.006	-0.010	<b>0.368</b>	<b>0.210</b>	<b>0.313</b>
Per_R_Amygdala/Hipp	0.106	-0.026	0.054	<b>0.415</b>	-0.102	<b>0.234</b>
Per_R_IntraparietalSulcus	-0.005	-0.032	0.034	<b>0.607</b>	-0.135	<b>0.431</b>
Per_L_AngularGyrus	<b>0.191</b>	-0.127	-0.007	<b>0.464</b>	0.084	0.186
Per_R_AngularGyrus	0.069	-0.189	-0.035	<b>0.386</b>	<b>-0.206</b>	<b>0.344</b>
Per_L_Fusiform	<b>-0.164</b>	-0.074	<b>0.132</b>	-0.061	0.081	<b>0.710</b>
Per_L_Pre/PostCentral	0.082	0.017	<b>0.218</b>	<b>0.361</b>	<b>0.181</b>	<b>0.249</b>
Per_L_SPG/Precuneus	<b>-0.124</b>	-0.003	0.063	0.078	<b>0.123</b>	<b>0.637</b>
Per_L_Precuneus	-0.077	0.076	-0.072	0.093	<b>0.295</b>	<b>0.593</b>
Ang_L_Insula/IFG	0.091	<b>0.096</b>	-0.046	<b>0.767</b>	<b>0.109</b>	<b>-0.275</b>
Ang_R_dmPFC/SFG	-0.065	0.006	-0.063	<b>0.803</b>	0.034	-0.152
Ang_R_Insula/IFG	<b>0.121</b>	<b>0.115</b>	-0.115	<b>0.736</b>	0.109	-0.195
Ang_L_OFC	-0.039	-0.097	0.041	<b>0.552</b>	<b>0.175</b>	<b>-0.295</b>
Ang_L_Fusiform	-0.032	-0.064	0.028	<b>-0.160</b>	<b>0.556</b>	<b>0.313</b>
Ang_L_MOG/V2	-0.120	0.031	-0.030	-0.099	<b>0.690</b>	<b>0.156</b>
Ang_R_PCC/Precuneus	0.015	0.056	0.019	-0.011	<b>0.813</b>	0.060
Ang_R_Precentral/ROL	-0.051	-0.108	<b>0.152</b>	0.027	<b>0.738</b>	<b>-0.098</b>
Ang_L_STG/STS	0.024	<b>-0.122</b>	<b>0.220</b>	0.034	<b>0.736</b>	<b>-0.097</b>
Ang_L_Calcarine/Retrospl	0.069	-0.005	0.074	<b>-0.130</b>	<b>0.747</b>	0.042
Ang_R_PCC/MidCingulate	-0.086	<b>-0.098</b>	0.007	-0.025	<b>0.822</b>	0.017
Ang_L_PostCentral	<b>0.172</b>	0.066	0.023	<b>0.303</b>	<b>0.671</b>	0.011
Ang_R_PostCentral	0.001	0.091	-0.103	0.062	<b>0.757</b>	-0.012
Ang_R_Calcarine/Retrospl	0.107	0.147	<b>-0.326</b>	<b>-0.353</b>	<b>0.421</b>	0.208

*Note.* Significant factor loadings are listed in bold font ( $p < .05$ ). R = right hemisphere, L = left hemisphere, Diff = contrast of neural activity during gaze vs. gender conditions, Per = parametric modulation by participants' individual perception/behavioral endorsement of stimuli as self-directed vs. averted, Ang = parametric modulation by objective gaze angle, All = contrast of neural activity across both task conditions vs. baseline, IFG = inferior frontal gyrus, IPL = inferior parietal lobule, dmPFC = dorsomedial prefrontal cortex, SMA = supplementary motor

area, STG = superior temporal gyrus, STS = superior temporal sulcus, TPJ = temporoparietal junction, V5 = middle temporal visual area, IOG = inferior occipital gyrus, OFC = orbitofrontal cortex, MOG = middle occipital gyrus, V2 = secondary visual cortex, dlPFC = dorsolateral prefrontal cortex, SFG = superior frontal gyrus, PCC = posterior cingulate cortex, vmPFC = ventromedial prefrontal cortex, ACC = anterior cingulate cortex, mPFC = medial prefrontal cortex, Hipp = hippocampus, SPG = superior parietal gyrus, MOG = middle occipital gyrus, ROL = Rolandic operculum, Retrospl = retrosplenial cortex.

**Table S5***Group Moderation of Associations between Social Cognition and Neural Factors*

Neural Factor	Social Cognition		Gaze Perception Width		Gaze Perception Threshold	
	$\beta$	$p$	$\beta$	$p$	$\beta$	$p$
Task activation	<b>.331</b>	<b>&lt; .001</b>	-.091	.379	<b>.306</b>	<b>.008</b>
Task activation x Group	<b>.321</b>	<b>&lt; .001</b>	-.111	.271	<b>.237</b>	<b>.034</b>
Gaze > Gender	<b>.159</b>	<b>.025</b>	-.041	.601	.006	.947
Gaze > Gender x Group	.132	.061	.073	.354	.064	.457
Gender > Gaze	<b>.186</b>	<b>.009</b>	-.040	.612	<b>.200</b>	<b>.024</b>
Gender > Gaze x Group	.086	.222	-.036	.649	-.098	.259
Direct gaze	.101	.153	<b>-.383</b>	<b>&lt; .001</b>	<b>.311</b>	<b>&lt; .001</b>
Direct gaze x Group	-.017	.811	-.044	.559	-.027	.748
Objectively averted gaze	-.015	.833	<b>-.352</b>	<b>&lt; .001</b>	<b>.228</b>	<b>.008</b>
Objectively averted gaze x Group	-.054	.436	-.089	.236	.006	.941
Perceived averted gaze	-.067	.387	<b>-.249</b>	<b>.004</b>	.139	.139
Perceived averted gaze x Group	-.123	.112	.031	.716	.038	.687
Diagnostic group (HC = 0, SZ = 1)	<b>-.471</b>	<b>&lt; .001</b>	<b>.149</b>	<b>.045</b>	-.006	.939

*Note.* N = 148 (77 SZ, 71 HC).  $\beta$  coefficients vary slightly from those presented in Figure 5, given the inclusion of interaction terms and differences in model estimation methods (ordinary least squares estimation with estimated factor scores vs. weighted least squares estimation in *MPLUS*).

**Table S6***Fit Indices for Follow-up Models*

Model	RMSEA	95% C.I.	TLI	CFI
S16. Behavioral with covariates	.019	[.000, .058]	.992	.995
S17. Behavioral without outliers	.034	[.000, .084]	.978	.987
S18. Behavioral with reduced SCog variable	.000	[.000, .055]	1.000	1.000
S19. Neural with covariates	.022	[.013, .029]	.908	.923
S20. Neural without outliers	.021	[.010, .029]	.923	.935
S21. Neural with reduced SCog variable	.027	[.018, .034]	.891	.909

*Note.* Model S18 was just identified, so fit indices should not be interpreted. All other models were over identified.

**Table S7**

*Group Moderation of Associations between Social Cognition and Neural Factors (Controlling for Age, Sex, Cognitive Ability, and Dataset Subsample)*

Neural Factor	Social Cognition		Gaze Width		Gaze Threshold	
	$\beta$	$p$	$\beta$	$p$	$\beta$	$p$
	Task activation	<b>.298</b>	<b>.002</b>	-.063	.433	<b>.256</b>
Task activation x Group	<b>.289</b>	<b>.002</b>	-.129	.117	.183	.115
Gaze > Gender	.102	.170	.066	.300	-.067	.456
Gaze > Gender x Group	.081	.272	.015	.811	.004	.964
Gender > Gaze	<b>.148</b>	<b>.044</b>	.040	.526	.173	.055
Gender > Gaze x Group	.087	.220	-.084	.174	.107	.220
Direct Gaze	.096	.214	<b>-.157</b>	<b>.018</b>	<b>.314</b>	<b>&lt; .001</b>
Direct Gaze x Group	-.024	.723	.006	.917	-.042	.606
Objectively averted gaze	.009	.909	<b>-.206</b>	<b>.002</b>	<b>.275</b>	<b>.003</b>
Objectively averted gaze x Group	.066	.340	<b>-.146</b>	<b>.014</b>	.001	.993
Perceived averted gaze	.056	.492	-.036	.598	-.137	.163
Perceived averted gaze x Group	.135	.086	.103	.124	-.013	.892
Diagnostic Group (HC = 0, SZ = 1)	<b>-.410</b>	<b>&lt; .001</b>	.105	.093	.075	.393

*Note.* N = 148 (77 SZ, 71 HC).  $\beta$  coefficients vary slightly from those presented in Figure S19 given the inclusion of interaction terms and differences in model estimation methods (ordinary least squares estimation with estimated factor scores vs. weighted least squares estimation in *MPLUS*).

**Table S8**

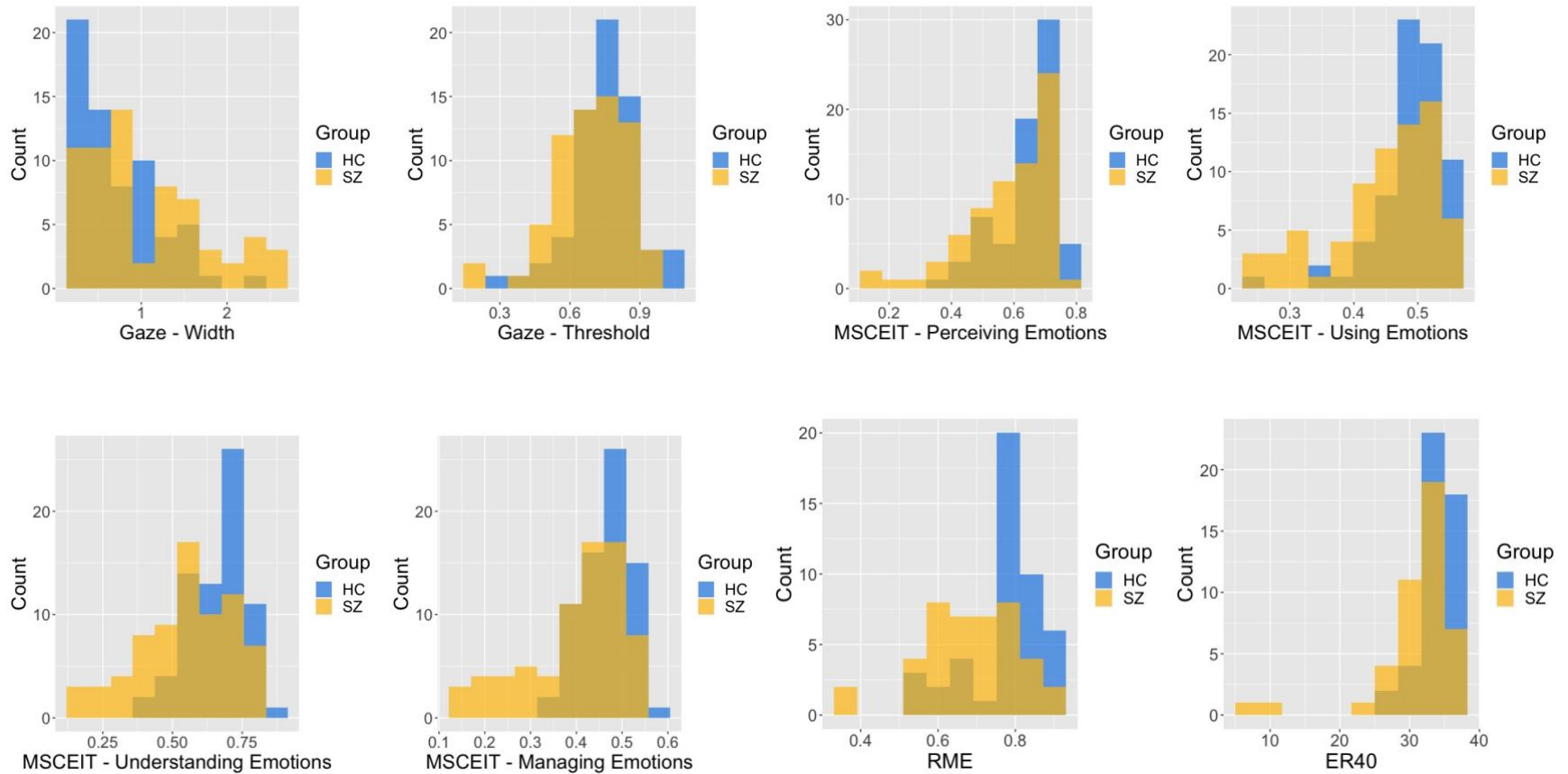
*Group Moderation of Associations between Social Cognition and Neural Factors (Removing Task-performance Outliers)*

Neural Factor	Social Cognition		Gaze Width		Gaze Threshold	
	$\beta$	$p$	$\beta$	$p$	$\beta$	$p$
	Task activation	<b>.312</b>	<b>&lt; .001</b>	-.091	.379	<b>.306</b>
Task activation x Group	<b>.314</b>	<b>&lt; .001</b>	-.111	.271	<b>.237</b>	<b>.034</b>
Gaze > Gender	<b>.149</b>	<b>.033</b>	-.041	.601	.006	.947
Gaze > Gender x Group	.135	.053	.073	.354	.064	.457
Gender > Gaze	<b>.189</b>	<b>.008</b>	-.040	.612	<b>.200</b>	<b>.024</b>
Gender > Gaze x Group	.076	.274	-.036	.649	-.098	.259
Direct Gaze	.101	.147	<b>-.383</b>	<b>&lt; .001</b>	<b>.311</b>	<b>&lt; .001</b>
Direct Gaze x Group	-.049	.476	-.044	.559	-.027	.748
Objectively averted gaze	-.045	.514	<b>-.352</b>	<b>&lt; .001</b>	<b>.228</b>	<b>.008</b>
Objectively averted gaze x Group	-.092	.174	-.089	.236	.006	.941
Perceived averted gaze	-.027	.726	<b>-.249</b>	<b>.004</b>	.139	.139
Perceived averted gaze x Group	-.093	.222	.031	.716	.038	.687
Diagnostic Group (HC = 0, SZ = 1)	<b>-.503</b>	<b>&lt; .001</b>	<b>.149</b>	<b>.045</b>	-.006	.939

*Note.* N = 148 (77 SZ, 71 HC). Sample size is equal to that reported in our primary analyses, as only individual outlier datapoints were removed rather than entire cases.  $\beta$  coefficients vary slightly from those presented in Figure S20, given the inclusion of interaction terms and differences in model estimation methods (ordinary least squares estimation with estimated factor scores vs. weighted least squares estimation in *MPLUS*).

**Figure S1**

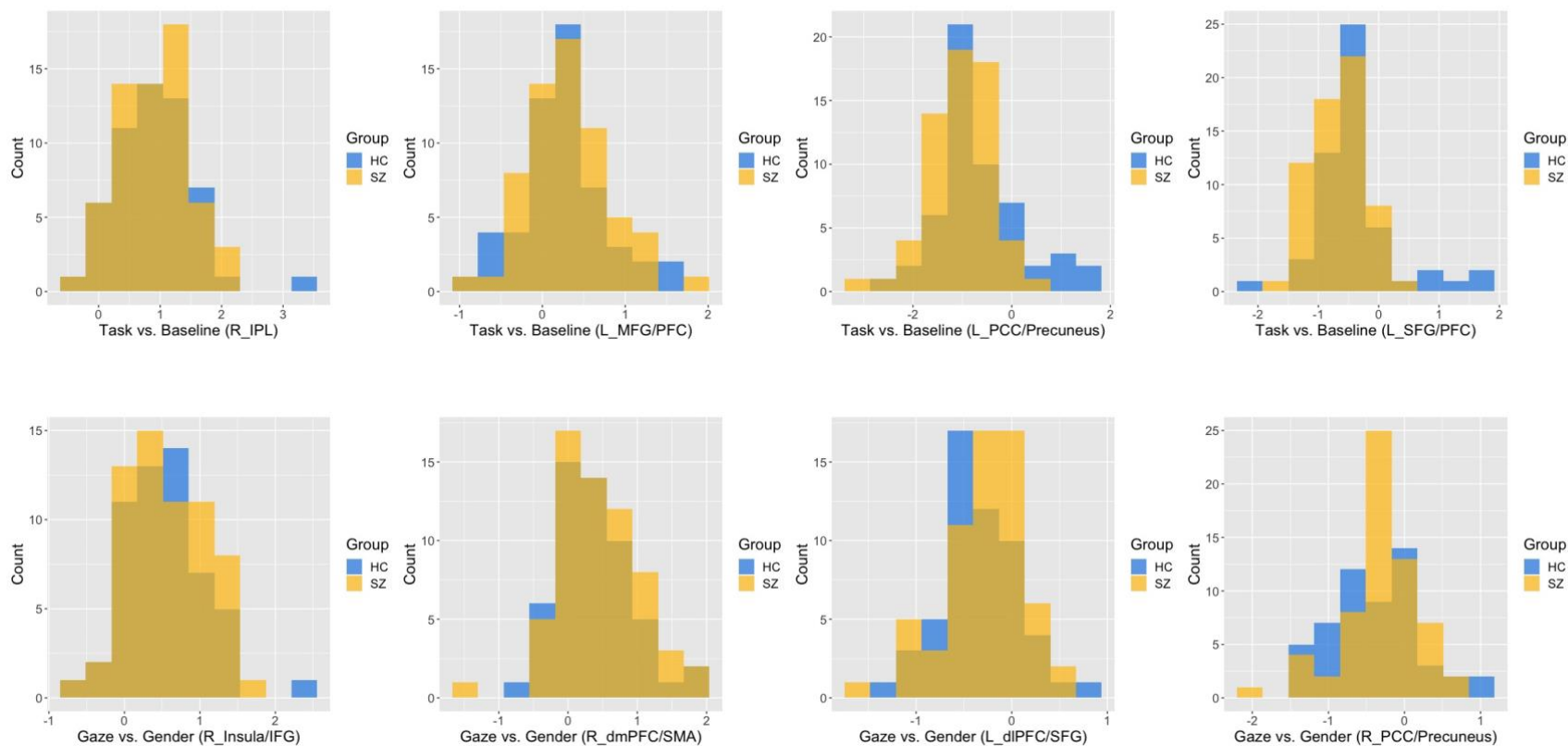
*Distributions of Social Cognition Variables*



*Note.* MSCEIT = Mayer-Salovey-Caruso Emotional Intelligence Test, ER40 = Penn Emotion Recognition Task, RME = Reading the Mind in the Eyes Test.

**Figure S2**

*Distributions for Representative Neural Variables (Task vs. Baseline and Gaze vs. Gender Contrasts)*

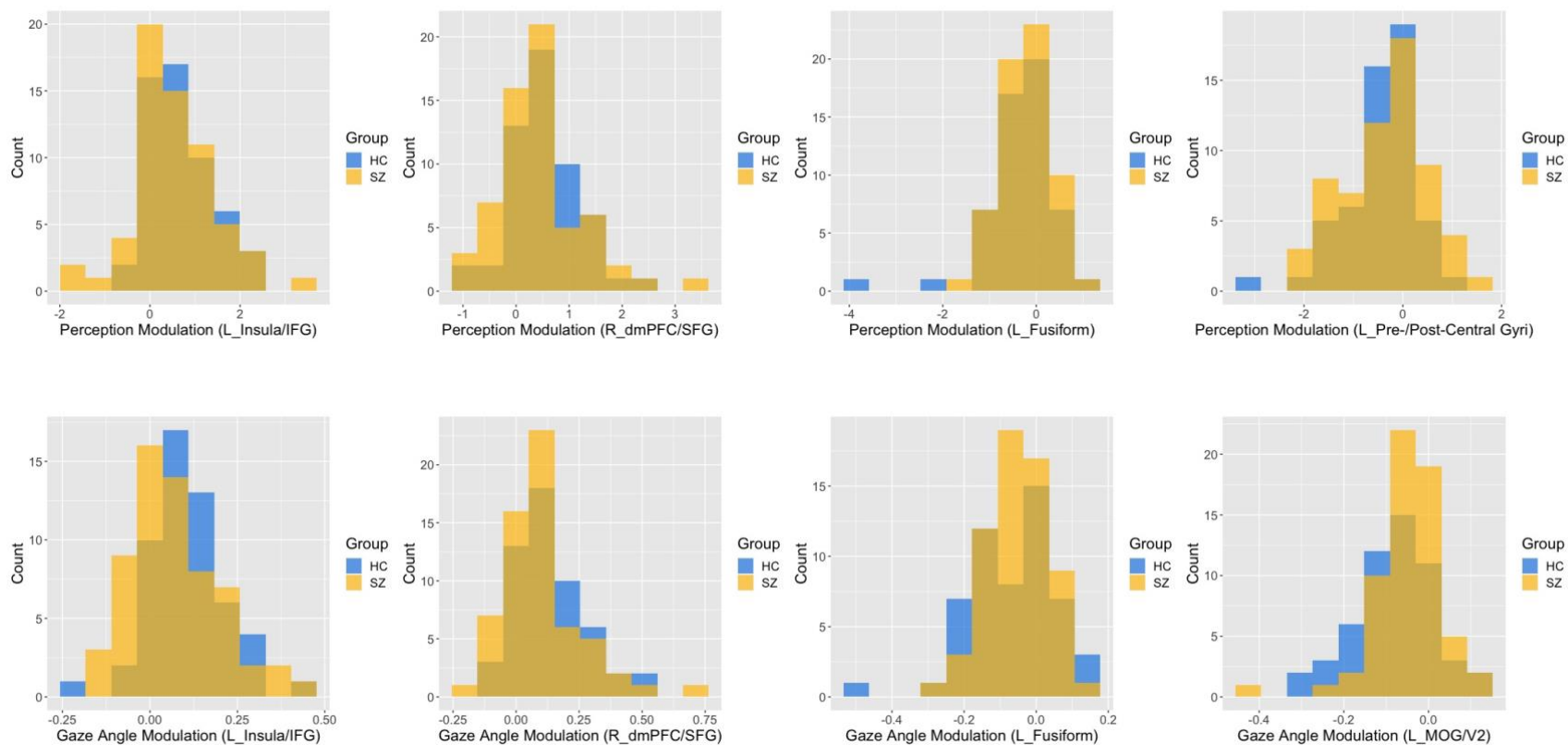


*Note.* L = left hemisphere, R = right hemisphere, IPL = inferior parietal lobule, MFG = middle frontal gyrus, PFC = prefrontal cortex, PCC = posterior cingulate cortex, SFG = superior frontal gyrus, IFG = inferior frontal gyrus, dmPFC = dorsomedial prefrontal cortex, SMA = supplementary motor area, dIPFC = dorsolateral prefrontal cortex



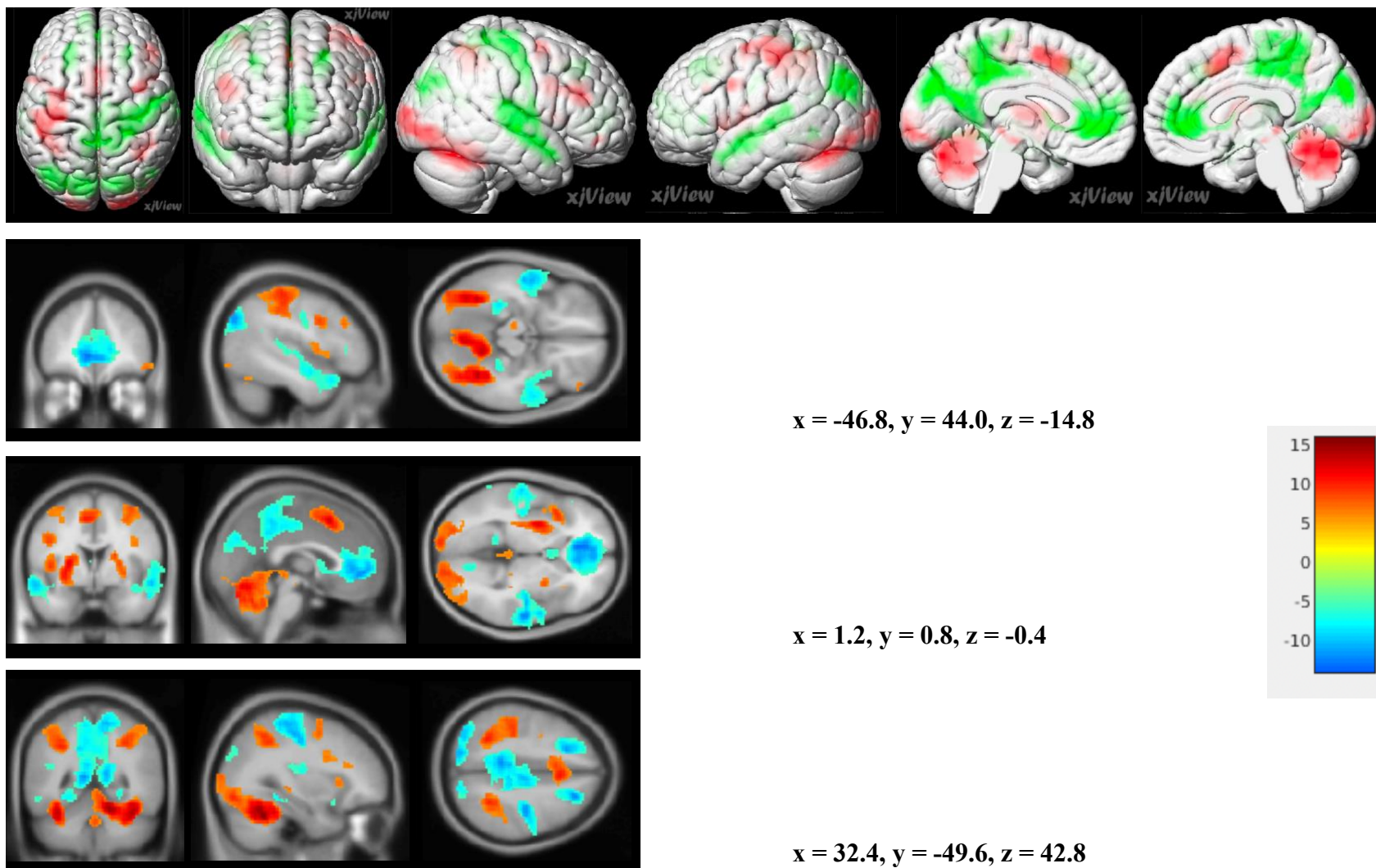
**Figure S3**

*Distributions for Representative Neural Variables (Modulation Contrasts)*



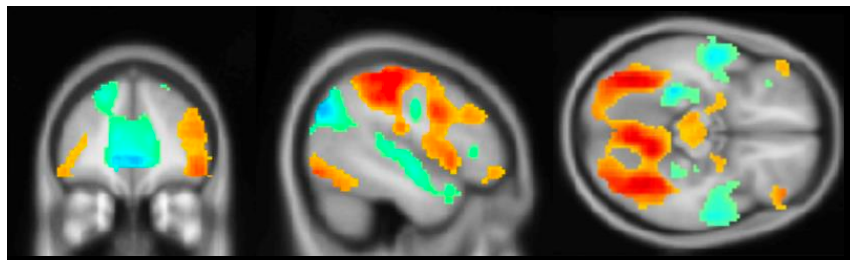
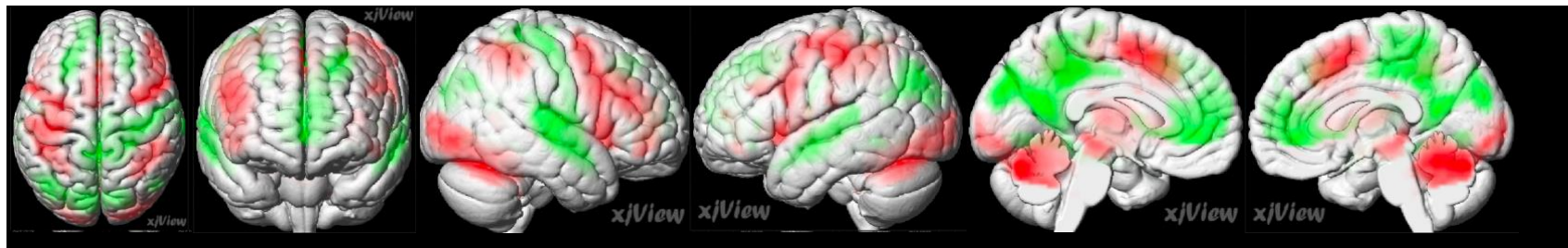
*Note.* L = left hemisphere, R = right hemisphere, IFG = inferior frontal gyrus, dmPFC = dorsomedial prefrontal cortex, SFG = superior frontal gyrus, MOG = middle occipital gyrus, V2 = secondary visual cortex

**Figure S4.** Whole-Sample Neural Activation across All Trials vs. Baseline

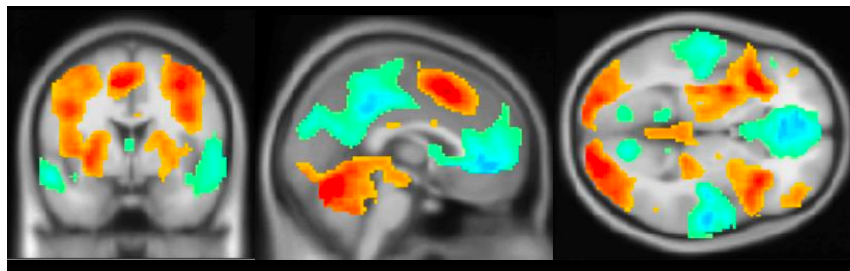


*Note.* Red = regions showing greater activation during the task vs. baseline. Blue/green = regions showing lower activation during the task vs. baseline. Color bar represents t-statistic at each voxel. Maps are based on an initial cluster-defining threshold of  $p < .001$  and FWE correction of  $p < .05$ .

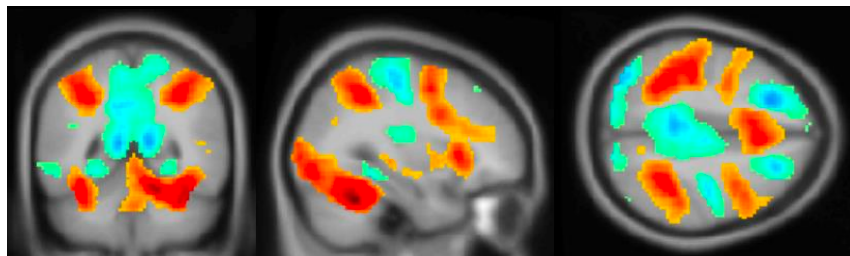
**Figure S5.** *Whole-Sample Neural Activation for Gaze Trials vs. Baseline*



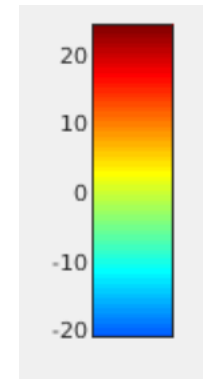
$x = -46.8, y = 44.0, z = -14.8$



$x = 1.2, y = 0.8, z = -0.4$

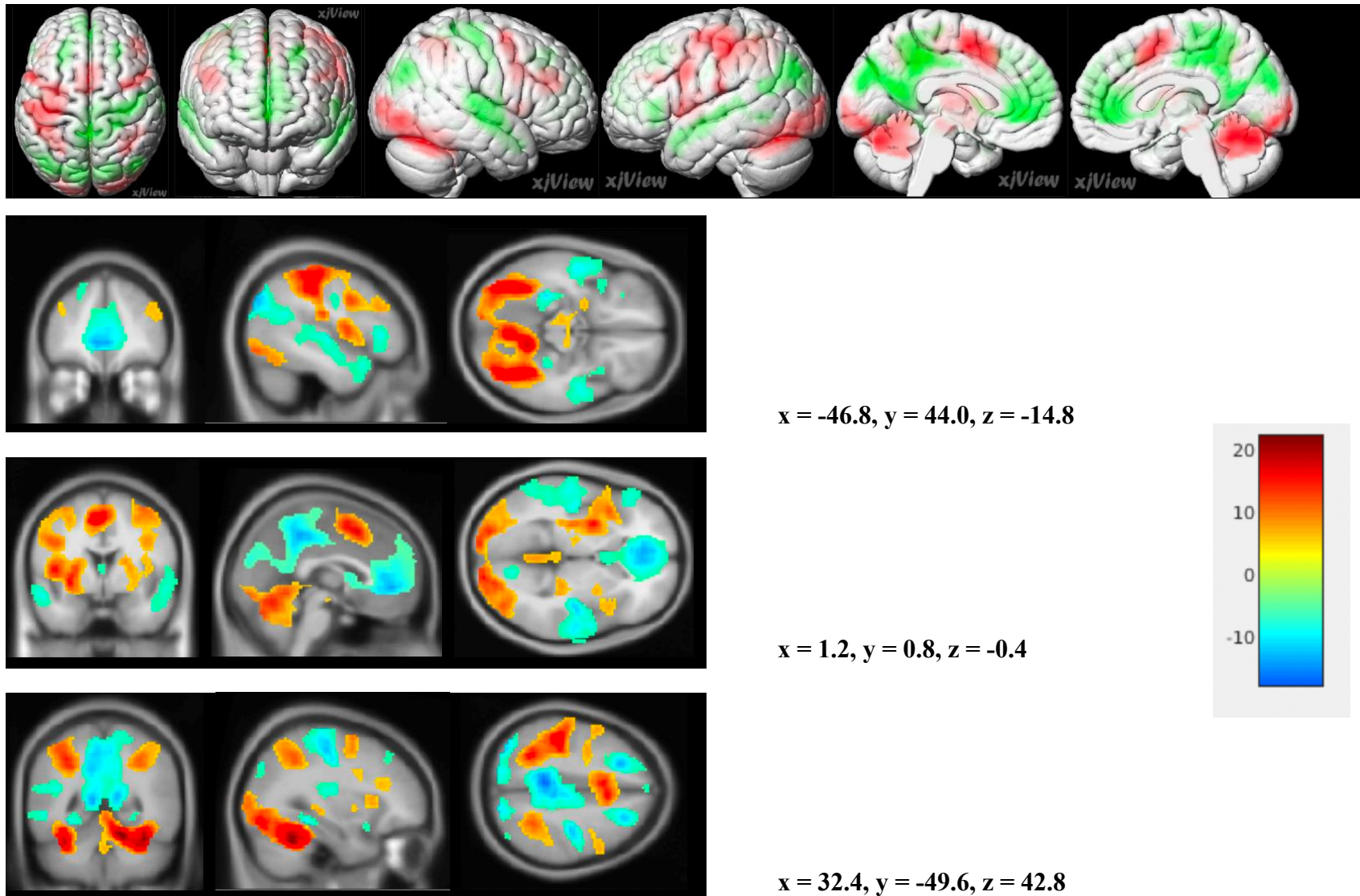


$x = 32.4, y = -49.6, z = 42.8$



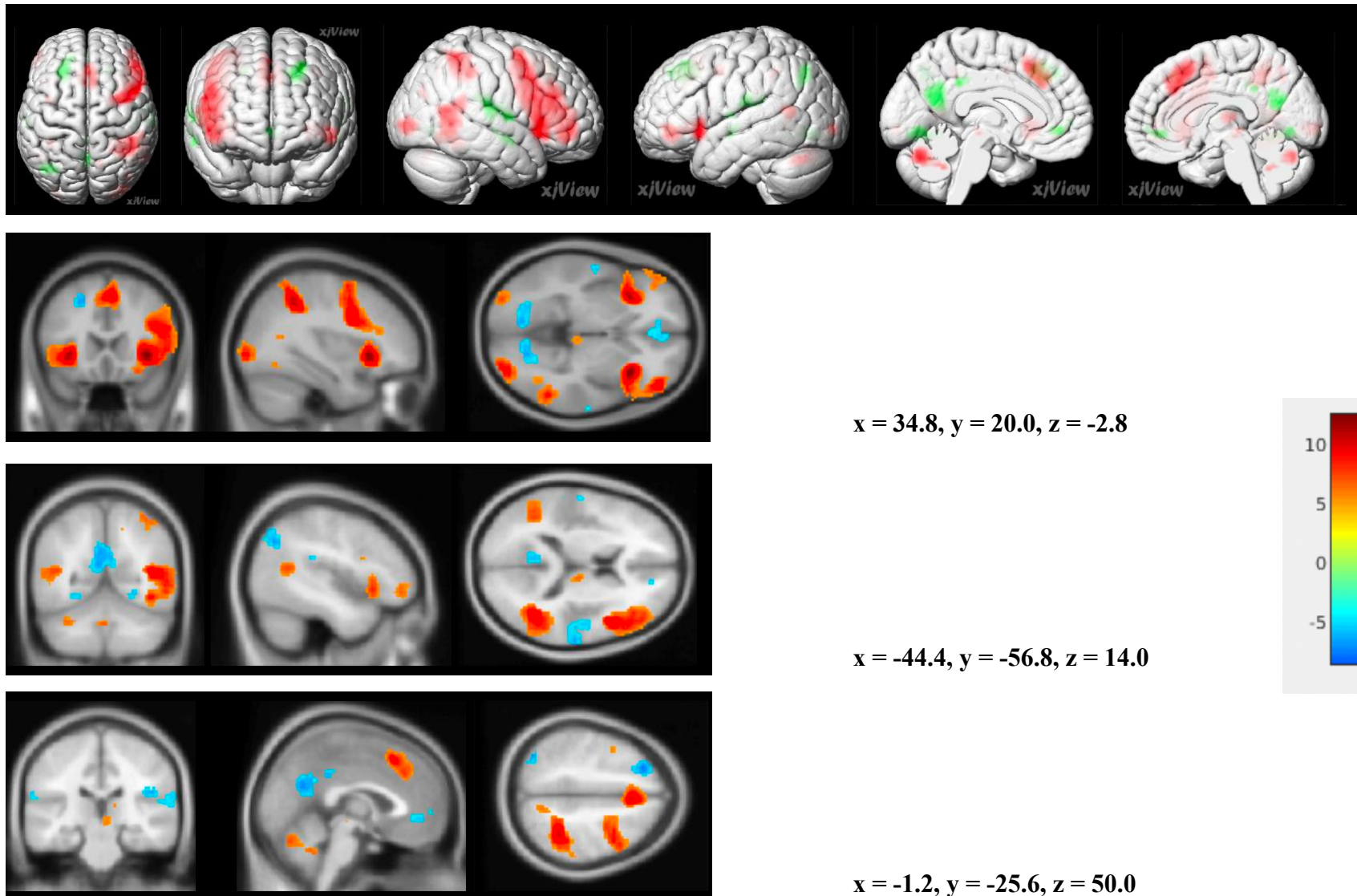
*Note.* Red = regions showing greater activation during gaze trials vs. baseline. Blue/green = regions showing lower activation during gaze trials vs. baseline. Color bar represents t-statistic at each voxel. Maps are based on an initial cluster-defining threshold of  $p < .001$  and FWE correction of  $p < .05$ .

**Figure S6.** *Whole-Sample Neural Activation for Gender Trials vs. Baseline*

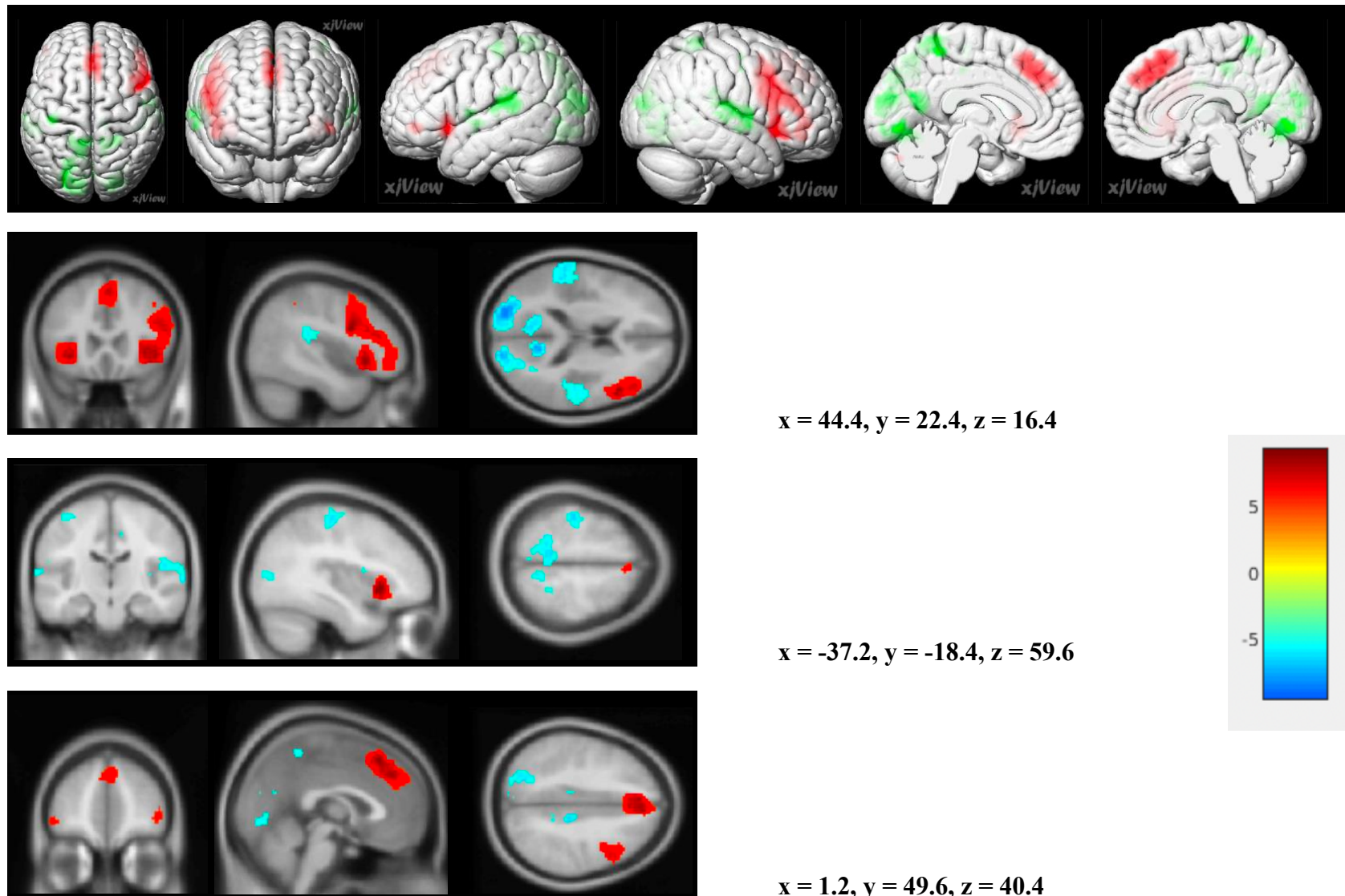


*Note.* Red = regions showing greater activation during gender trials vs. baseline. Blue/green = regions showing lower activation during gender trials vs. baseline. Color bar represents t-statistic at each voxel. Maps are based on an initial cluster-defining threshold of  $p < .001$  and FWE correction of  $p < .05$ .

**Figure S7.** Whole-Sample Preferential Neural Activation for Gaze vs. Gender

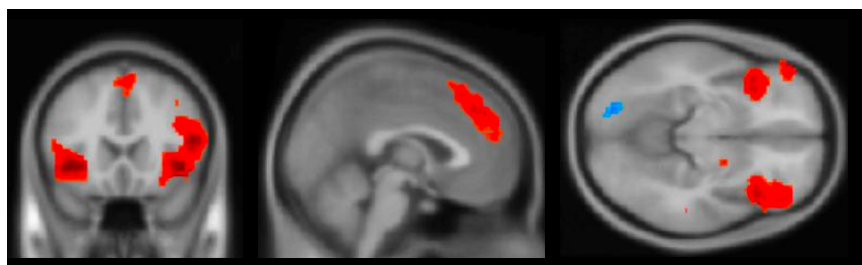
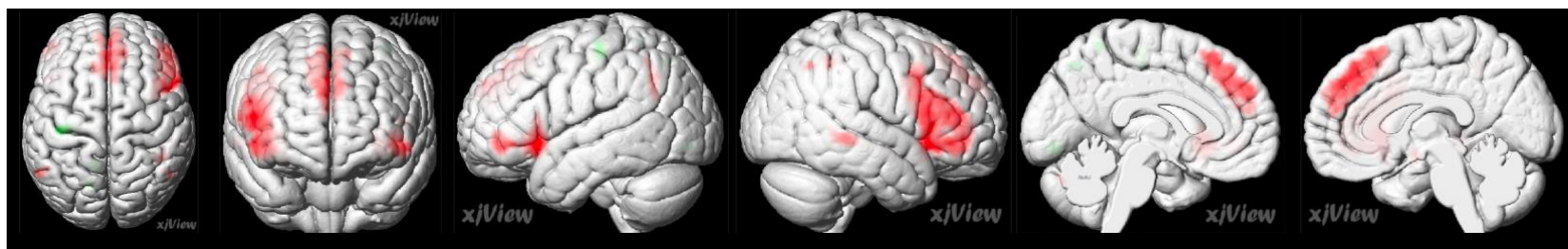


*Note.* Red = regions showing greater activation during gaze vs. gender. Blue/green = regions showing greater activation during gender vs. gaze. Color bar represents t-statistic at each voxel. Maps are based on an initial cluster-defining threshold of  $p < .001$  and FWE correction of  $p < .05$ .

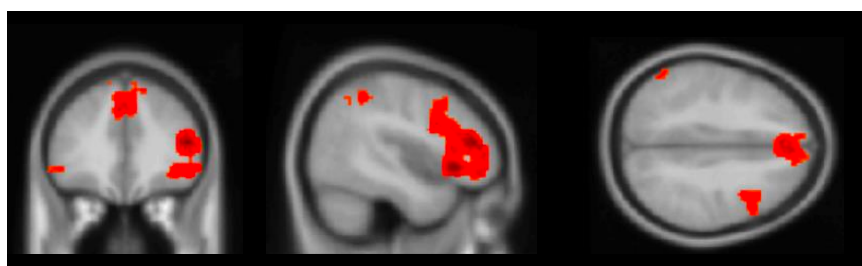
**Figure S8.** *Whole-Sample Modulation of Neural Activation by Objective Gaze Angle*

*Note.* Red = regions showing greater activation when stimulus gaze is more direct. Blue/green = regions showing greater activation when stimulus gaze is more averted. Color bar represents t-statistic at each voxel. Maps are based on an initial cluster-defining threshold of  $p < .001$  and FWE correction of  $p < .05$ .

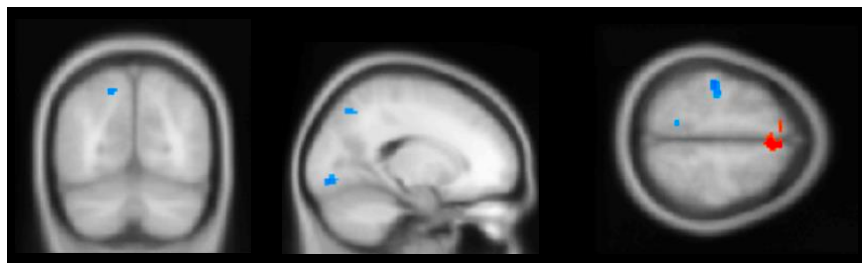
**Figure S9.** *Whole-Sample Modulation of Neural Activation by Participants' Perception/Behavioral Endorsement*



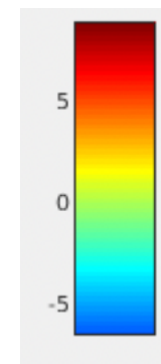
**x = -1.2, y = 20.0, z = -10.0**



**x = 44.4, y = 34.4, z = 38.0**



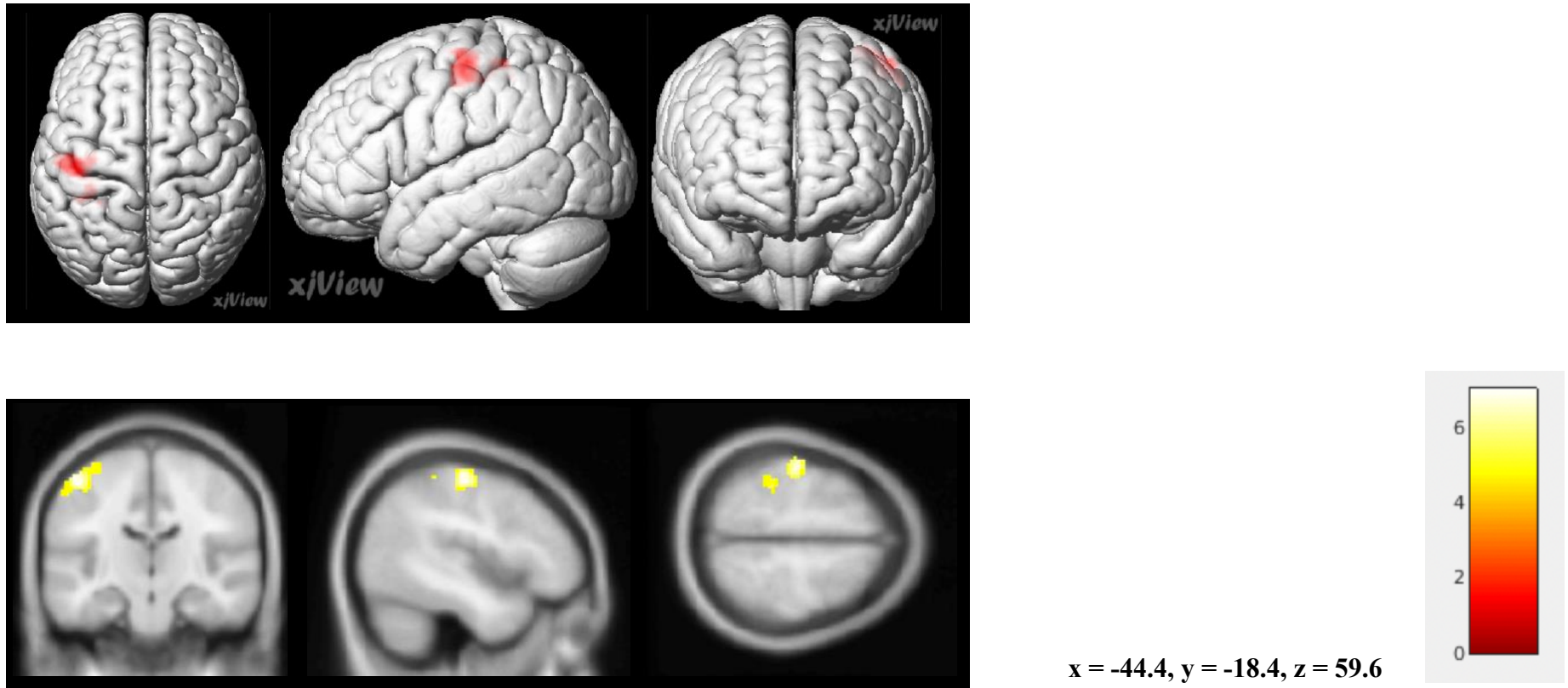
**x = -17.2, y = -68.6, z = 59.6**



*Note.* Red = regions showing greater activation when gaze is endorsed as direct. Blue/green = regions showing greater activation when gaze is endorsed as averted. Color bar represents t-statistic at each voxel. Maps are based on an initial cluster-defining threshold of  $p < .001$  and FWE correction of  $p < .05$ .

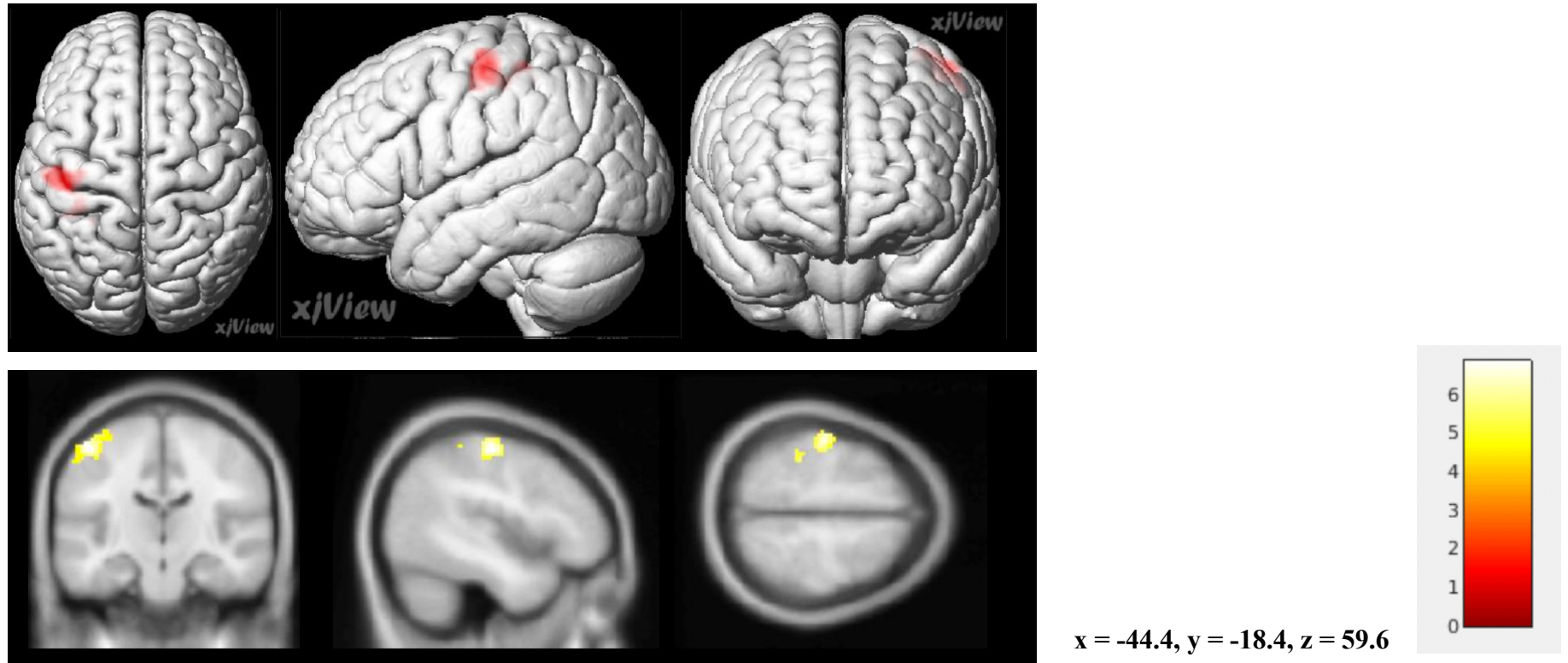
**Figure S10**

*Group Differences in Neural Activation for All Trials vs. Baseline*

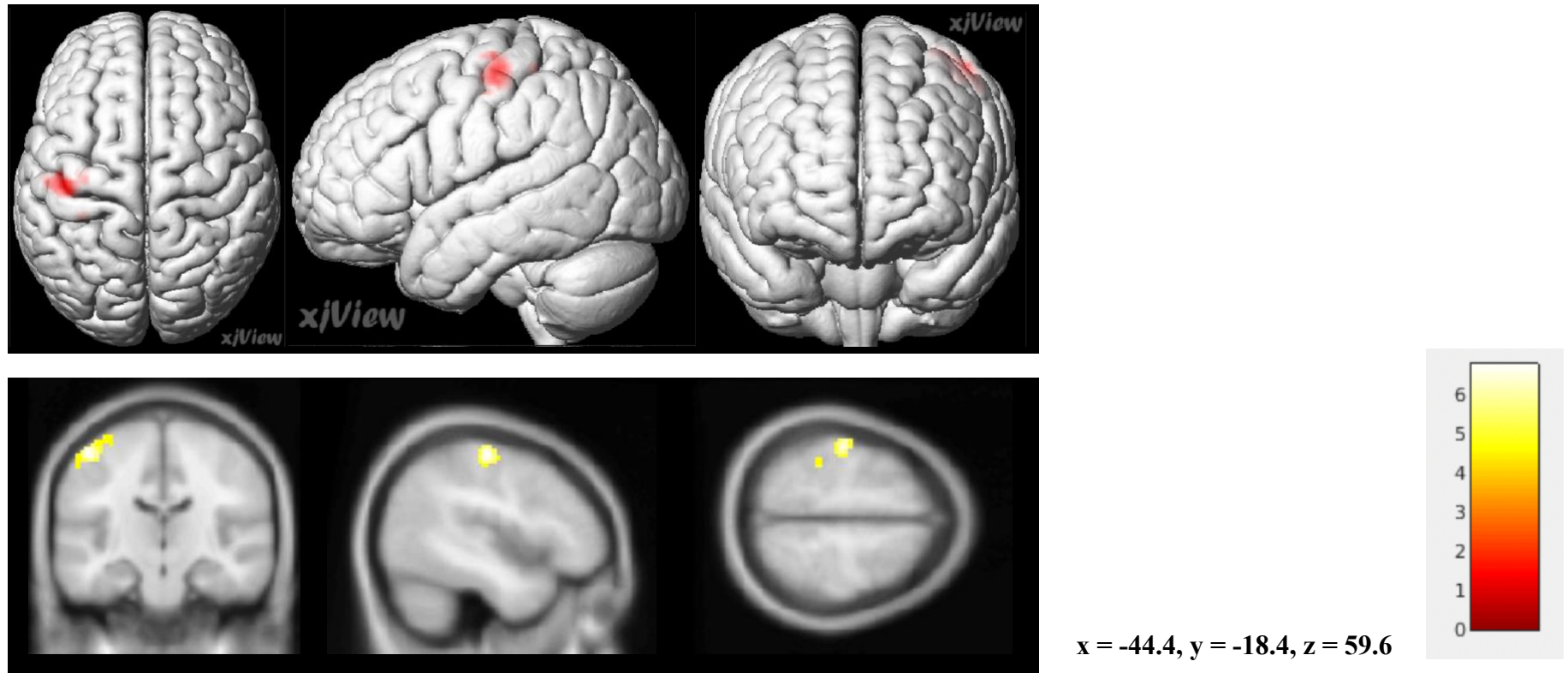


*Note.* Yellow/Red = regions showing greater activation across all trials (vs. baseline) in SZ vs. HC participants. Color bar represents t-statistic at each voxel. Maps are based on an initial cluster-defining threshold of  $p < .001$  and FWE correction of  $p < .05$ .

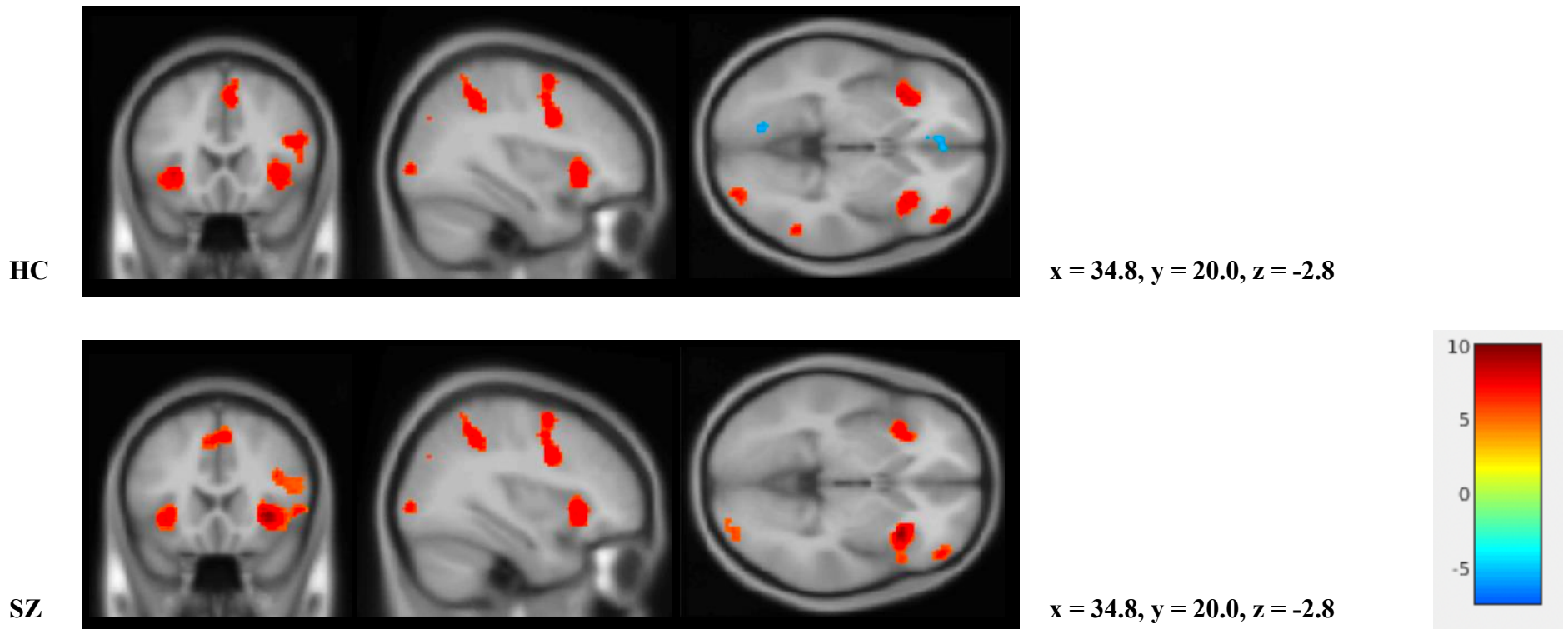


**Figure S11***Group Differences in Neural Activation for Gaze Trials vs. Baseline*

*Note.* Yellow/Red = regions showing greater activation during gaze trials (vs. baseline) in SZ vs. HC participants. Color bar represents t-statistic at each voxel. Maps are based on an initial cluster-defining threshold of  $p < .001$  and FWE correction of  $p < .05$ .

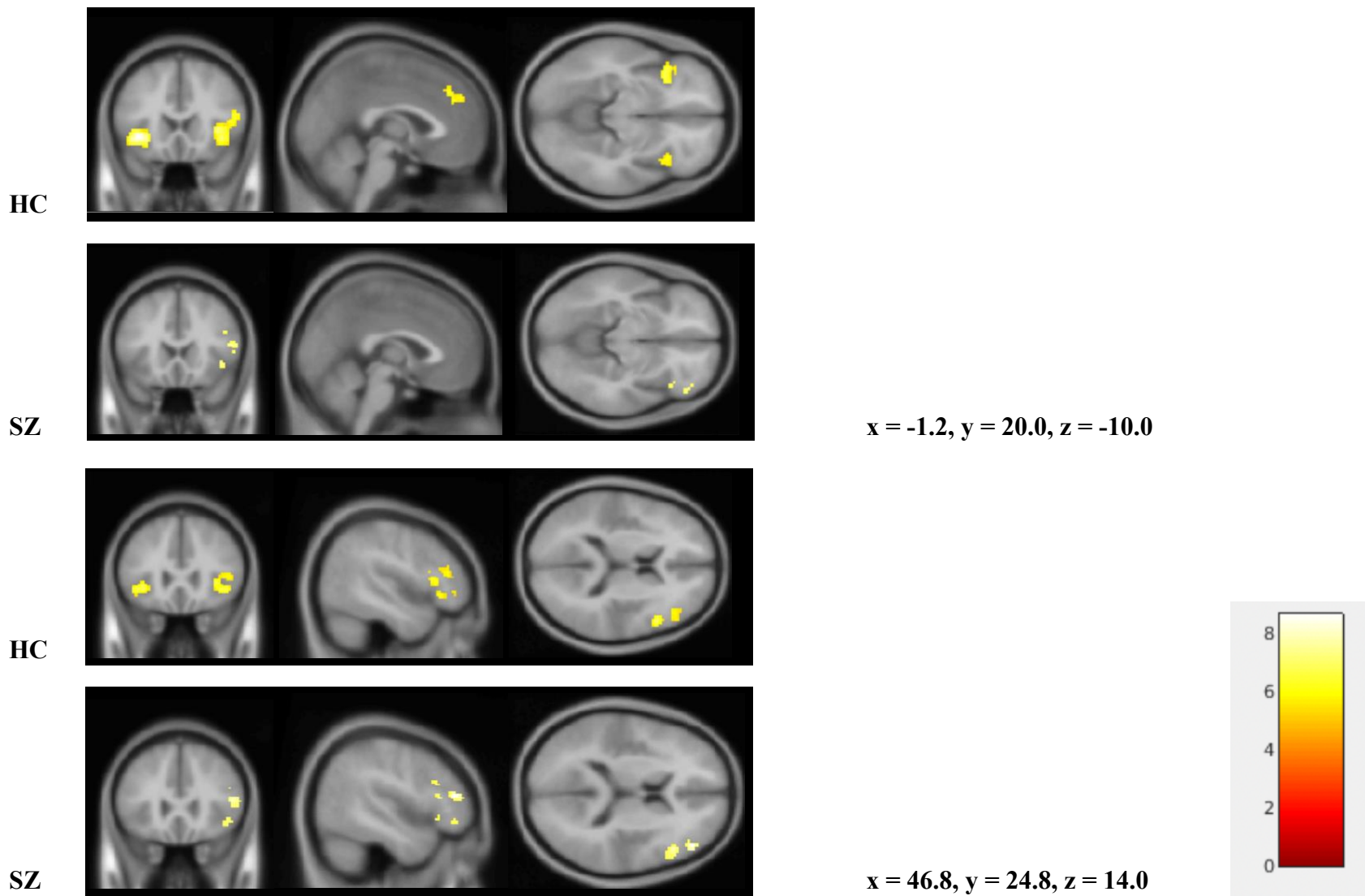
**Figure S12***Group Differences in Neural Activation for Gender Trials vs. Baseline*

*Note.* Yellow/Red = regions showing greater activation during gender trials (vs. baseline) in SZ vs. HC participants. Color bar represents t-statistic at each voxel. Maps are based on an initial cluster-defining threshold of  $p < .001$  and FWE correction of  $p < .05$ .

**Figure S13***Group Maps of Preferential Neural Activation for Gaze vs. Gender*

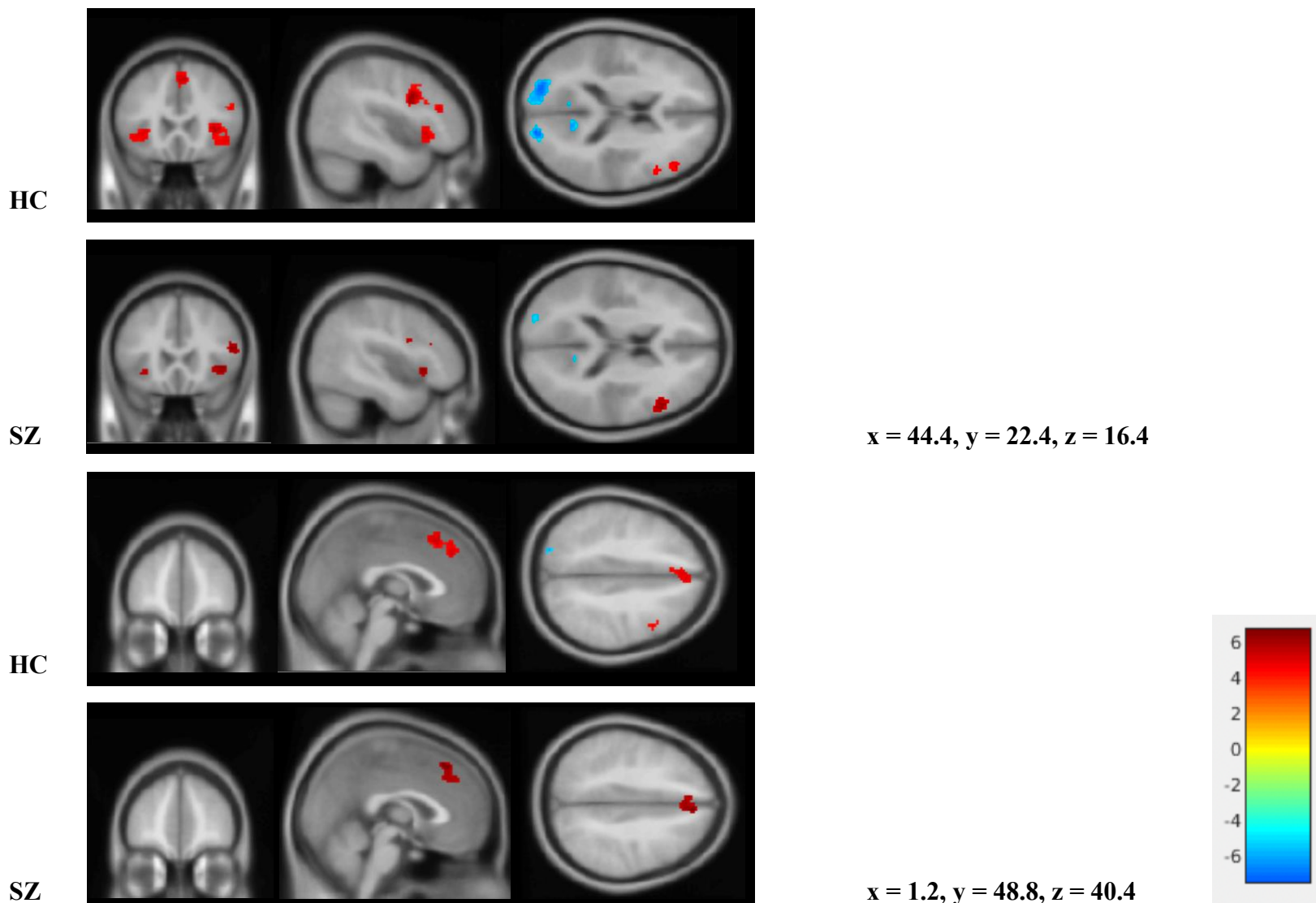
*Note.* Red = regions showing greater activation during gaze vs. gender. Blue = regions showing greater activation during gender vs. gaze. Color bar represents t-statistic at each voxel. Maps are based on an initial cluster-defining threshold of  $p < .001$  and FWE correction of  $p < .05$ .

**Figure S14.** *Group Maps of Modulation of Neural Activation by Participants' Perception/Behavioral Endorsement*



*Note.* Yellow = regions showing greater activation when participants endorsed gaze stimuli as self-directed. Color bar represents t-statistic at each voxel. Maps are based on an initial cluster-defining threshold of  $p < .001$  and FWE correction of  $p < .05$ .

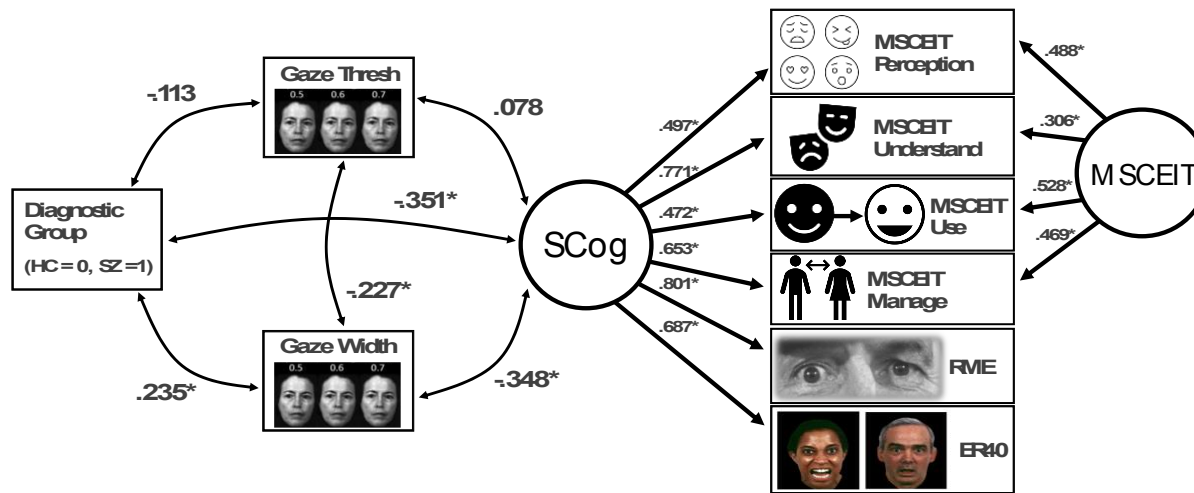
**Figure S15.** *Group Maps of Modulation of Neural Activation by Objective Gaze Angle*



*Note.* Red = regions showing greater activation when stimulus gaze is more direct. Blue/green = regions showing greater activation when stimulus gaze is more averted. Color bar represents t-statistic at each voxel. Maps are based on an initial cluster-defining threshold of  $p < .001$  and FWE correction of  $p < .05$ .

**Figure S16**

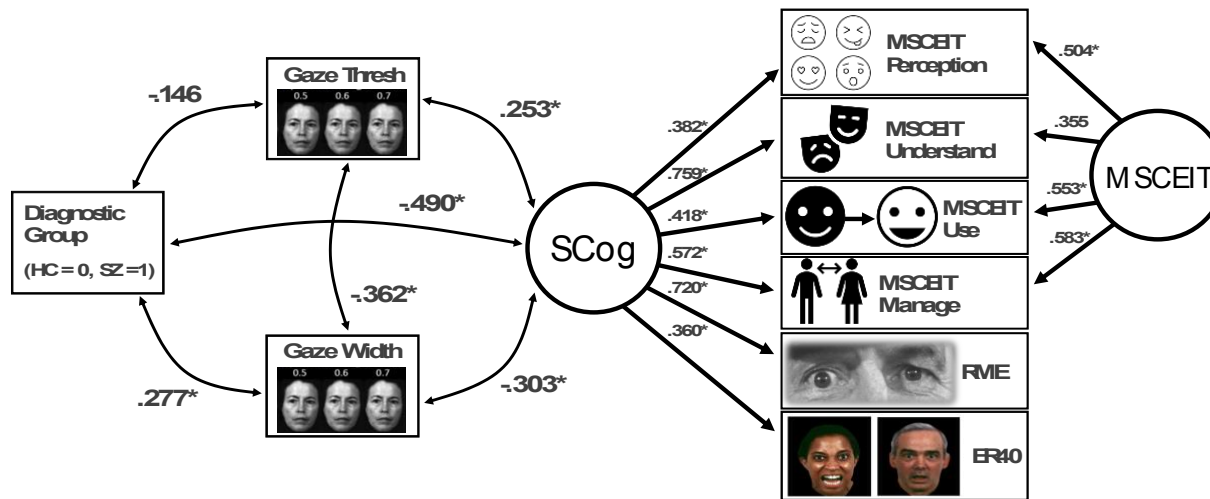
*Behavioral Model of Diagnosis, Gaze Perception, and Latent Social Cognition (Controlling for Age, Sex, Cognitive Ability, and Dataset Subsample)*



*Note.* MSCEIT = Mayer-Salovey-Caruso Emotional Intelligence Test, RME = Reading the Mind in the Eyes Test, ER-40 = Penn Emotion Recognition Test. The model depicts associations among diagnostic group, gaze perception metrics, and social cognition; the model differs from the one presented in the main text (Figure 3), as age, sex, cognitive ability, and dataset subsample were included as covariates. Factor loadings for a social cognition latent factor (SCog) are shown on the right, as well as a method factor for the MSCEIT branch scores. Better social cognition was associated with greater perceptual precision. SZ showed worse social cognition and lower perceptual precision. \* $p < .05$ .

**Figure S17**

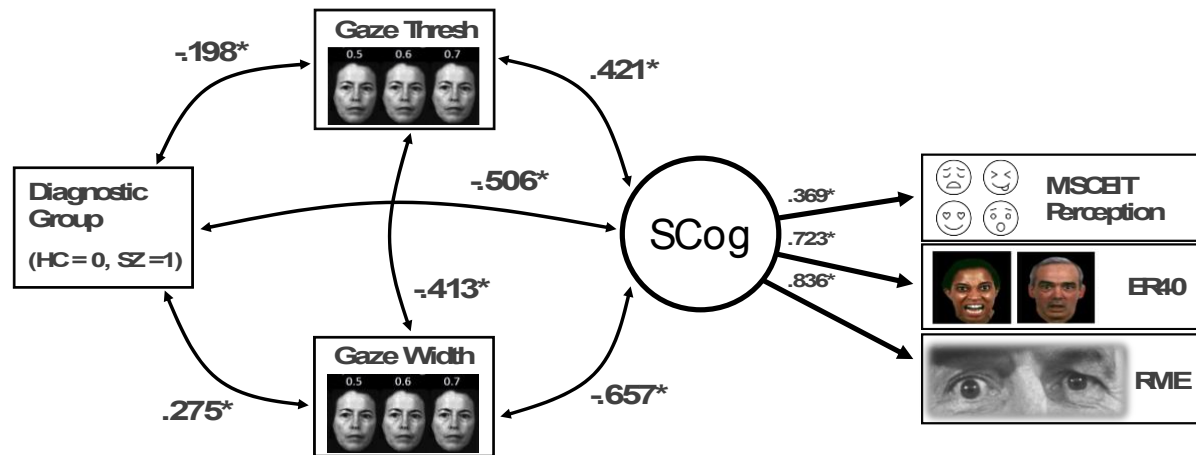
*Behavioral Model of Diagnosis, Gaze Perception, and Latent Social Cognition (Removing Task-performance Outliers)*



*Note.* MSCEIT = Mayer-Salovey-Caruso Emotional Intelligence Test, RME = Reading the Mind in the Eyes Test, ER-40 = Penn Emotion Recognition Test. The model depicts associations among diagnostic group, gaze perception metrics, and social cognition; the model differs from the one presented in the main text (Figure 3), as outliers on task performance variables identified using a Rosner’s test were removed. Factor loadings for a social cognition latent factor (SCog) are shown on the right, as well as a method factor for the MSCEIT branch scores. Better social cognition was associated with greater perceptual precision and lower self-referential bias. SZ showed worse social cognition and lower perceptual precision. \* $p < .05$ .

**Figure S18**

*Behavioral Model of Diagnosis, Gaze Perception, and Latent Social Cognition (Using Only the Perception Branch Score from the MSCEIT)*

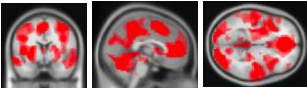
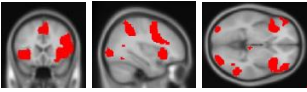
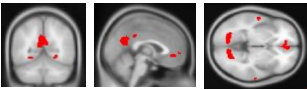
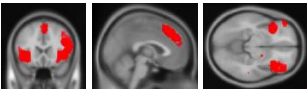
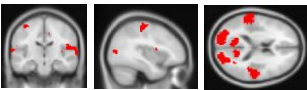
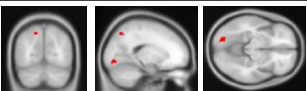


**Note.** MSCEIT = Mayer-Salovey-Caruso Emotional Intelligence Test, RME = Reading the Mind in the Eyes Test, ER-40 = Penn Emotion Recognition Test. The model depicts associations among diagnostic group, gaze perception metrics, and social cognition; the model differs from the one presented in the main text (Figure 3), as only the perceiving emotions branch score from the MSCEIT was included. Factor loadings for a social cognition latent factor (SCog) are shown on the right. Better social cognition was associated with greater perceptual precision and lower self-referential bias. SZ showed worse social cognition, lower perceptual precision, and higher self-referential bias.  $*p < .05$ .



**Figure S19**

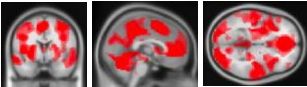
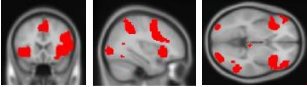
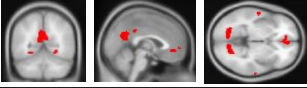
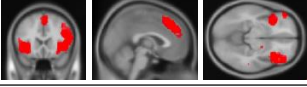
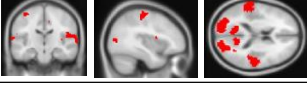

*Whole-sample Regression Coefficients among Key Study Variables (Controlling for Age, Sex, Cognitive Ability, and Dataset Subsample)*

		Group (SZ = 1)	Social Cognition	Gaze Threshold	Gaze Width
Task Activation		<b>-.196*</b>	<b>.223*</b>	.125	-.040
Gaze > Gender		.139	<b>.255**</b>	-.032	.092
Gender > Gaze		.055	<b>.245*</b>	<b>.187*</b>	-.026
Self-directed Gaze		.012	.085	<b>.273**</b>	-.095
Objectively Averted Gaze		<b>-.242*</b>	-.049	<b>.212</b>	<b>-.160*</b>
Perceived Averted Gaze		.071	-.109	.050	-.035

*Note.* The figure displays standardized path coefficients from each of the neural factors to criterion variables for diagnostic group, latent social cognition, gaze threshold (i.e., self-referential bias), and gaze width (i.e., perceptual precision). Neural factors correspond to 1) global task activation vs. baseline, 2) preferential activation for gaze (vs. gender), 3) preferential activation for gender (vs. gaze), 4) modulation (increase) of activation by perception of stimuli as self-directed and by viewing stimuli with objectively more self-directed gaze angles, 5) modulation (increase) of activation by viewing objectively more averted gaze angles, and 6) modulation (increase) of activation by perception of stimuli as averted. Voxel clusters that were more active in response to self-directed gaze—including those from the fMRI contrast for participant perception/behavioral endorsement and the contrast for objective gaze angle—loaded onto factor 4, whereas voxel clusters that were more active in response to averted gaze were split across factors 5 (for the objective gaze angle contrast) and 6 (for the participant perception/behavioral endorsement contrast). Significant positive associations are colored in red and negative correlations in blue. The model differs from the one presented in the main text (Figure 5), as age, sex, cognitive ability, and dataset subsample were included as covariates. \* $p < .05$ , \*\* $p < .01$ .

**Figure S20**

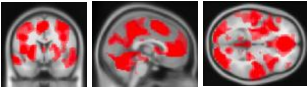
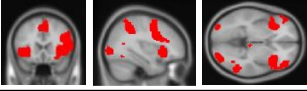
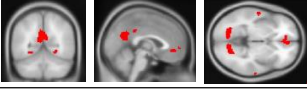
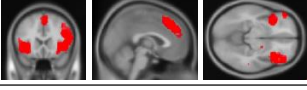
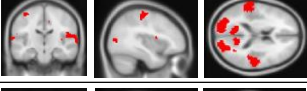
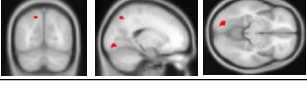
*Whole-sample Regression Coefficients among Key Study Variables (Removing Task-performance Outliers)*

		Group (SZ = 1)	Social Cognition	Gaze Threshold	Gaze Width
Task Activation		<b>-.210*</b>	<b>.211*</b>	<b>.202*</b>	<b>-.037</b>
Gaze > Gender		<b>-.035</b>	<b>.233*</b>	<b>-.033</b>	<b>-.003</b>
Gender > Gaze		<b>-.057</b>	<b>.225*</b>	<b>.151</b>	<b>-.042</b>
Self-directed Gaze		<b>-.043</b>	<b>.075</b>	<b>.175*</b>	<b>-.365**</b>
Objectively Averted Gaze		<b>-.186</b>	<b>-.065</b>	<b>.240**</b>	<b>-.355**</b>
Perceived Averted Gaze		<b>.106</b>	<b>-.085</b>	<b>.059</b>	<b>-.199*</b>

*Note.* The figure displays standardized path coefficients from each of the neural factors to criterion variables for diagnostic group, latent social cognition, gaze threshold (i.e., self-referential bias), and gaze width (i.e., perceptual precision). Neural factors correspond to 1) global task activation vs. baseline, 2) preferential activation for gaze (vs. gender), 3) preferential activation for gender (vs. gaze), 4) modulation (increase) of activation by perception of stimuli as self-directed and by viewing stimuli with objectively more self-directed gaze angles, 5) modulation (increase) of activation by viewing objectively more averted gaze angles, and 6) modulation (increase) of activation by perception of stimuli as averted. Voxel clusters that were more active in response to self-directed gaze—including those from the fMRI contrast for participant perception/behavioral endorsement and the contrast for objective gaze angle—loaded onto factor 4, whereas voxel clusters that were more active in response to averted gaze were split across factors 5 (for the objective gaze angle contrast) and 6 (for the participant perception/behavioral endorsement contrast). Significant positive associations are colored in red and negative correlations in blue. The model differs from the one presented in the main text (Figure 5), as outliers on task performance variables identified using a Rosner's test were removed. \* $p < .05$ , \*\* $p < .01$ .

**Figure S21**

*Whole-sample Regression Coefficients among Key Study Variables (Using Only the Perception Branch Score from the MSCEIT)*

		Group (SZ = 1)	Social Cognition	Gaze Threshold	Gaze Width
Task Activation		<b>-.208*</b>	.168	.122	-.036
Gaze > Gender		-.027	.230	.007	-.010
Gender > Gaze		-.051	<b>.297*</b>	<b>.192*</b>	-.046
Self-directed Gaze		-.045	.031	<b>.321*</b>	<b>-.371**</b>
Objectively Averted Gaze		-.188	.038	<b>.225**</b>	<b>-.356**</b>
Perceived Averted Gaze		.104	-.123	.062	<b>-.203*</b>

*Note.* The figure displays standardized path coefficients from each of the neural factors to criterion variables for diagnostic group, latent social cognition, gaze threshold (i.e., self-referential bias), and gaze width (i.e., perceptual precision). Neural factors correspond to 1) global task activation vs. baseline, 2) preferential activation for gaze (vs. gender), 3) preferential activation for gender (vs. gaze), 4) modulation (increase) of activation by perception of stimuli as self-directed and by viewing stimuli with objectively more self-directed gaze angles, 5) modulation (increase) of activation by viewing objectively more averted gaze angles, and 6) modulation (increase) of activation by perception of stimuli as averted. Voxel clusters that were more active in response to self-directed gaze—including those from the fMRI contrast for participant perception/behavioral endorsement and the contrast for objective gaze angle—loaded onto factor 4, whereas voxel clusters that were more active in response to averted gaze were split across factors 5 (for the objective gaze angle contrast) and 6 (for the participant perception/behavioral endorsement contrast). Significant positive associations are colored in red and negative correlations in blue. The model differs from the one presented in the main text (Figure 5), as only the perceiving emotions branch score from the MSCEIT, the RME, and the ER-40 were included as indicators of social cognition. \* $p < .05$ , \*\* $p < .01$ .